

AD _____

Award Number: W81XWH-05-2-0011

TITLE: ~~Development of a novel, non-invasive, non-pharmacological method to predict the onset of hypoxia in patients with chronic heart failure~~

PRINCIPAL INVESTIGATOR: ~~Dr. Mark A. Tuck~~

CONTRACTING ORGANIZATION: ~~University of Colorado at Denver, Department of Medicine, Division of Pulmonary, Critical Care and Sleep Medicine, and the Pulmonary and Critical Care Research Institute, Aurora, CO~~
~~University of Colorado Health Sciences Center, Aurora, CO~~

REPORT DATE: ~~10/15/2007~~

TYPE OF REPORT: Annual

PREPARED FOR: U.S. Army Medical Research and Materiel Command
Fort Detrick, Maryland 21702-5012

DISTRIBUTION STATEMENT: Approved for public release; distribution unlimited

The views, opinions and/or findings contained in this report are those of the author(s) and should not be construed as an official Department of the Army position, policy or decision unless so designated by other documentation.

REPORT DOCUMENTATION PAGE

Form Approved
OMB No. 0704-0188

Public reporting burden for this collection of information is estimated to average 1 hour per response, including the time for reviewing instructions, searching existing data sources, gathering and maintaining the data needed, and completing and reviewing this collection of information. Send comments regarding this burden estimate or any other aspect of this collection of information, including suggestions for reducing this burden to Department of Defense, Washington Headquarters Services, Directorate for Information Operations and Reports (0704-0188), 1215 Jefferson Davis Highway, Suite 1204, Arlington, VA 22202-4302. Respondents should be aware that notwithstanding any other provision of law, no person shall be subject to any penalty for failing to comply with a collection of information if it does not display a currently valid OMB control number. **PLEASE DO NOT RETURN YOUR FORM TO THE ABOVE ADDRESS.**

1. REPORT DATE (DD-MM-YYYY) 01-03-2011	2. REPORT TYPE Annual	3. DATES COVERED (From - To) 1 Mar 2010 - 28 Feb 2011		
4. TITLE AND SUBTITLE Control of Disease Recurrence by Tumor-Infiltrating T Cells in Ovarian Cancer		5a. CONTRACT NUMBER		
		5b. GRANT NUMBER W81XWH-09-1-0169		
		5c. PROGRAM ELEMENT NUMBER		
6. AUTHOR(S) Brad Nelson E-Mail: bnelson@bccancer.bc.ca		5d. PROJECT NUMBER		
		5e. TASK NUMBER		
		5f. WORK UNIT NUMBER		
7. PERFORMING ORGANIZATION NAME(S) AND ADDRESS(ES) British Columbia Cancer Agency Vancouver, BC V5Z 1L3		8. PERFORMING ORGANIZATION REPORT NUMBER		
9. SPONSORING / MONITORING AGENCY NAME(S) AND ADDRESS(ES) U.S. Army Medical Research and Materiel Command Fort Detrick, Maryland 21702-5012		10. SPONSOR/MONITOR'S ACRONYM(S)		
		11. SPONSOR/MONITOR'S REPORT NUMBER(S)		
12. DISTRIBUTION / AVAILABILITY STATEMENT Approved for Public Release; Distribution Unlimited				
13. SUPPLEMENTARY NOTES				
14. ABSTRACT Ovarian cancer patients with large numbers of T cells in their tumor live longer after chemotherapy compared to patients with fewer T cells in their tumor. Our goal is to use modern genomic techniques to identify the antigens recognized by these T cells, with an emphasis on new antigens that arise during chemotherapy. To this end, we are collecting matched primary and recurrent tumor tissue from ovarian cancer patients (Tasks 1-2); this is progressing well. The antigen receptors expressed by tumor-infiltrating T cells (Task 2) and B cells (Task 3) have been identified in several patients by DNA sequencing methods. Primary and recurrent tumor tissue from one patient has been analyzed by whole exome sequencing, and a large number of candidate mutations have been identified (Task 4). Finally, new methods have been developed to rapidly test the recognition of tumor mutations by T cells from patients (Task 5). Overall, this project is progressing on schedule and is yielding publishable results and leveraged funding.				
15. SUBJECT TERMS Tumor immunology, immunotherapy, ovarian cancer, antibody, T cell, tumor antigen, mutation, next generation sequencing				
16. SECURITY CLASSIFICATION OF: a. REPORT U b. ABSTRACT U c. THIS PAGE U		17. LIMITATION OF ABSTRACT UU	18. NUMBER OF PAGES 36	19a. NAME OF RESPONSIBLE PERSON USAMRMC 19b. TELEPHONE NUMBER (include area code)

Table of Contents

	<u>Page</u>
Introduction.....	4
Body.....	4
Key Research Accomplishments.....	11
Reportable Outcomes.....	12
Conclusion.....	13
References.....	13
Appendices.....	13
Supporting Data.....	13

W81XWH-09-1-0169 (OC080380) Annual Report, March 2011

PI: Brad H. Nelson, Ph.D.

Co-PIs: Rob Holt, Ph.D., John Webb Ph.D., Peter Watson, M.D.

Title of Project: Control of Disease Recurrence by Tumor-Infiltrating T Cells in Ovarian Cancer

INTRODUCTION:

In epithelial ovarian cancer (EOC), tumor-infiltrating CD8+ T cells are strongly associated with increased progression-free and overall survival following chemotherapy. However, the antigens recognized by tumor-infiltrating T cells remain largely unknown. Furthermore, it is not clear how tumor-infiltrating T cells, having failed to prevent the primary tumor, can oppose tumor recurrence. Recent work has shown that chemotherapy, in the context of impaired DNA repair pathways, induces mutations in the cancer genome, some of which contribute to chemo-resistance. Chemotherapy-induced mutations may provide a new source of tumor antigens for T cells, since mutated or aberrantly expressed proteins should be perceived as "non-self". Based on these considerations, we hypothesize that the mutational effects of chemotherapy generate new tumor antigens that trigger a second wave of CD8+ T cell responses, which in turn promote favorable clinical outcomes. To test this hypothesis, we are using serological and genomic methods to identify the evolving repertoire of tumor antigens and T cell responses in EOC patients who demonstrate favorable clinical outcomes.

The study has five tasks:

Task 1. Collection and processing of biospecimens

Task 2. To determine whether chemotherapy induces the emergence of new tumor-associated CD8+ T cell clones in EOC.

Task 3. To identify by serological approaches tumor antigens induced by chemotherapy in EOC.

Task 4. To identify changes to the tumor transcriptome induced by chemotherapy in EOC.

Task 5. To determine whether tumor-associated CD8+ T cells in EOC recognize putative chemotherapy-induced antigens.

Significance. This will be the first study to test the hypothesis that the mutational effects of platinum/taxane-based chemotherapy generate novel antigens that stimulate host CD8+ T cell responses. With a better understanding of how T cell responses evolve during standard treatments, we believe it will be possible in future to prolong progression-free survival by enhancing the host T cell response using immunodulatory agents, vaccines or adoptively transferred T cells.

BODY:**Task 1. Collection and processing of biospecimens.**

This task concerns the collection of matched primary and recurrent ascites from 6 patients with high-grade serous ovarian cancer; isolation and storage of CD45+ leukocyte, CD8+ lymphocyte and CD45- tumor cell subfractions; and collection of blood samples before, during and after primary surgery and chemotherapy.

Progress to date:

To date, we have collected 12 matched primary and recurrent ascites tumor specimens. However, the main challenge has been to collect matched samples from women with a favorable progression-free interval (PFI) (ideally > 24 months); so far, only 1 of the 12 patients with matched primary and recurrent ascites samples meets the 24 month PFI. Fortunately, there are an additional 12 patients from whom we have collected primary ascites and who are “in the running” for a PFI > 24 months. We are making every effort to monitor these patients and collect recurrent ascites specimens as they become available. As for the other aspects of this task, we have developed methods to successfully isolate and store CD45+ leukocyte, CD8+ lymphocyte and CD45- tumor cell subfractions. Furthermore, we have a high success rate at collecting serial blood samples before, during and after primary surgery and chemotherapy. Thus, this task is proceeding as expected.

Task 2. To determine whether chemotherapy induces the emergence of new tumor-associated CD8+ T cell clones in EOC.

We proposed to study tumor-infiltrating T cells from primary and recurrent ascites to look for changes in T cell subsets (CD3, CD4, CD8), and various activation and differentiation markers. We also proposed to sequence T cell receptors (TCRs) to identify 10-20 predominant T cell clones from recurrent tumors. Serial blood and ascites samples would then be analyzed by QPCR with clonotype-specific primers to determine the time of emergence of these T cell clones. Our hypothesis predicts that a large proportion of CD8+ T cell clones present in recurrent ascites will have arisen during or after chemotherapy.

Progress to date:

We have started experiments for Task 2 using specimens from a patient (IROC024) who fell a few months short of our PFI criterion, but is nonetheless of great interest for several reasons: (a) we have collected primary ascites as well as matched ascites from her first, second and third recurrence; (b) there are ample vials of tumor cells available from each time point, so we can use these specimens to develop our methodology without fear of squandering precious samples; and (c) a full complement of serial blood samples is available for later experiments to track T cell clones over time. Using these specimens, we have successfully separated tumor cells, CD4+ T cells and CD8+ T cells by flow cytometry, and these samples were sent to Rob Holt's lab for RNA isolation and TCR sequencing.

To perform TCR sequencing, 5' Rapid Amplification of cDNA Ends (RACE) and PCR were used to amplify the antigen-binding regions of the TCRs. PCR products were cloned into plasmids for Sanger sequencing. 96 clones were sequenced, which yielded 36 TCR sequences. Five distinct clones were identified. A predominant T cell clonotype was found in the CD8+ fraction (24/36 clones), and a second predominant clonotype was found in the CD4+ fraction (8/36 clones). This is consistent with our hypothesis that tumor-infiltrating T cells in ovarian cancer represent antigen-specific, clonally expanded subpopulations.

The success of this experiment gives us confidence to perform TCR sequencing on a larger scale using Illumina sequencing and additional specimens. Currently, we have isolated RNA from ascites specimens collected from three time points (primary tumor, first relapse, second relapse) for three patients (IROC024, IROC002 and IROC012). The clinical course for IROC024 was shown in our 2010 annual report; this information is shown in **Figure 1** for patients IROC002 and IROC012. Construction of the 9 Illumina libraries required for TCR sequencing is underway. Furthermore, the method for Illumina library construction has been optimized by sample indexing (bar coding) to allow pooling of libraries prior to sequencing,

which reduces the chance of contaminating TCR sequences between samples and reduces the overall cost (Warren et al., *Genome Research*, 2011; **APPENDIX A**).

Finally, we have also developed methods based on multiparameter flow cytometry to analyze the functional responses of CD4+ and CD8+ T cells in the tumor environment (Tran et al. *PLoS One*, 2010). These methods will allow us to assess how the functional properties of tumor-reactive T cells change as patients undergo chemotherapy.

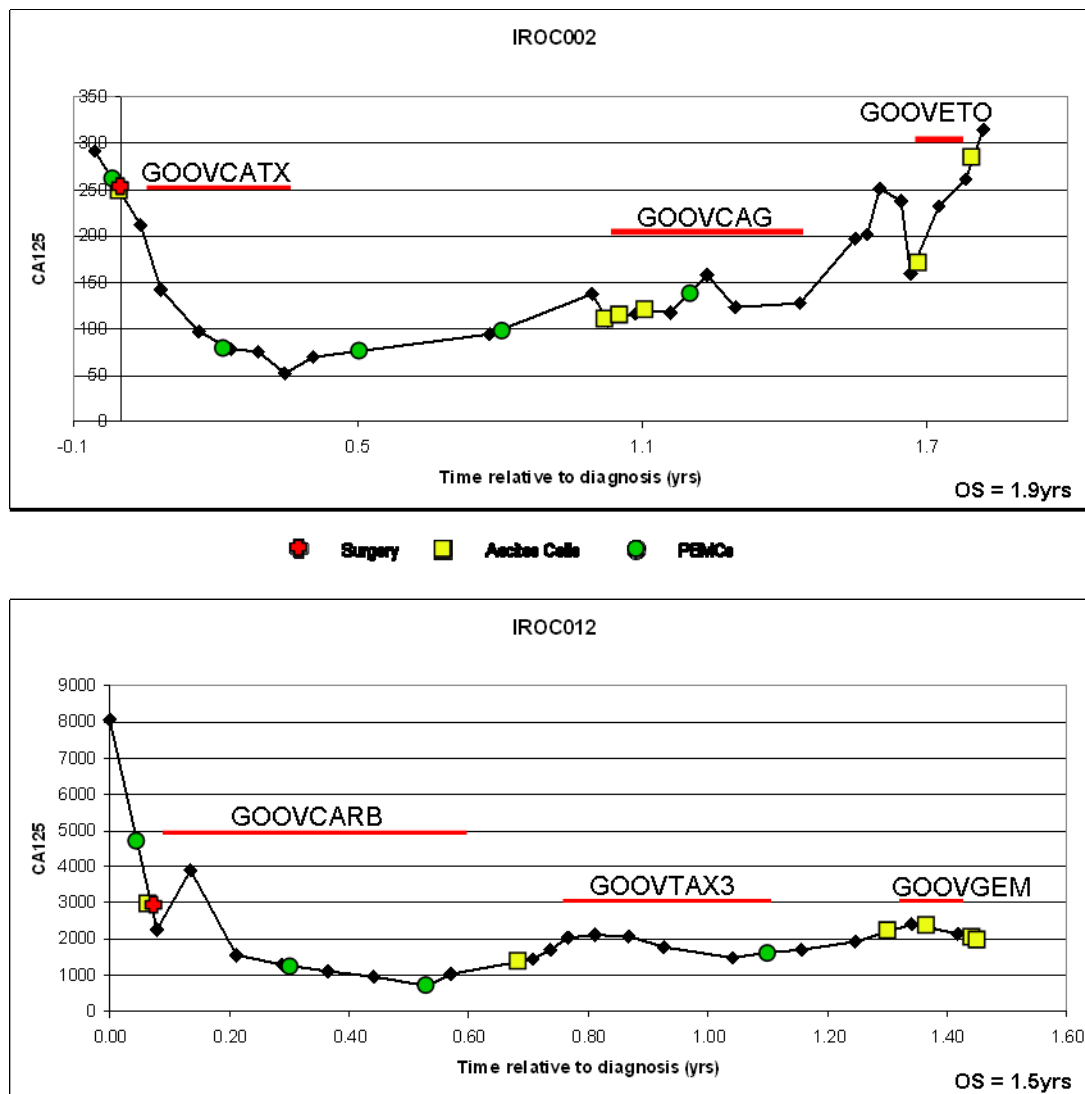


Figure 1. Clinical history and available specimens for IROC002 and IROC012, two high-grade serous ovarian cancer patients to be studied in Tasks 2 and 4. Tumor burden is indicated by CA125 measurements (Y axis) over time (X axis). Also shown are the time points at which ascites cells (yellow squares) and peripheral blood mononuclear cells (PMBC; green squares) were collected. Chemotherapy protocols are shown (GOOVCATX = carboplatin and paclitaxel;

GOOVCAG = carboplatin and gemcitabine; GOOVETO = etoposide; GOOVCARB = carboplatin alone; GOOVTAX3 = paclitaxel alone; GOOVGEM = gemcitabine alone). Note that ascites cells (containing tumor) were successfully collected from both patients at primary surgery, first recurrence, and second recurrence. Overall survival time is listed in the bottom right corner of each graph.

Task 3. To identify by serological approaches tumor antigens induced by chemotherapy in EOC.

In our original application, we proposed to construct autologous cDNA libraries in a yeast-based expression system using mRNA from recurrent ascites tumor cells. Libraries would then be screened with patient sera to identify tumor antigens recognized by IgG autoantibodies. For each antigen, we would determine whether expression is seen in the primary and/or recurrent tumor tissue (by QPCR); whether the antigen shows sequence alterations; and the clinical time point at which antibody responses develop. The overarching goal is to identify new antigens that arise during or after chemotherapy.

Progress to date: While we originally proposed to use serum autoantibodies to identify tumor antigens, we have decided instead to use autoantibodies derived from tumour-infiltrating B cells. This change of strategy was motivated by our finding that CD20+ tumour-infiltrating B cells (TIL-B) are associated with increased survival in high-grade serous ovarian cancer (**Fig. 2A**, from Milne 2009 *PLoS ONE* 4(7): e6412). Intrigued by this observation, Brad Nelson (PI) reviewed the literature concerning the role of TIL-B in other cancers (Nelson, B.H., *J. Immunology*, 2010; **APPENDIX B**). As described in the article, TIL-B are associated with patient survival in a wide variety of cancers. Moreover, in the setting of autoimmunity and allograft rejection (i.e., rejection of solid organ transplants), tissue-infiltrating B cells are associated with strong T cell responses against target tissues. B cells are thought to facilitate tumor/tissue destruction by producing antibodies; releasing cytokines and chemokines that attract T cells; or serving as antigen presenting cells for CD4+ and CD8+ T cells.

In the past year, we investigated these potential mechanisms in ovarian cancer. As a starting point, we wanted to determine if TIL-B are antigen-experienced, which would provide evidence they are responding to antigens expressed by tumor cells. To this end, we sequenced IgG heavy chain variable regions (including V, D, and J gene segments) from three ovarian cancers in which CD20+ TIL-B were present. We performed 6 independent PCRs using primer pairs designed to amplify VH1, VH2, VH3, VH4, VH5, and VH6 sequences. PCR reactions were combined in pools of two, cloned into a plasmid vector and transfected into *E. coli*. For each tumor, up to 96 bacterial colonies were subjected to capillary-based DNA sequencing.

This analysis of IgG sequences revealed several important points. First, IgG from TIL-B exhibited a high level of somatic hypermutation: on average 20 base pairs (bp) were mutated in each ~400 bp variable region, which resulted in an average of 13 amino acid (aa) substitutions per variable region (**Fig. 2B**). This is consistent with prior findings for antigen-experienced B cells (which show an average of 18 bp and 10 aa substitutions) and in stark contrast to naïve B cells (which show an average of 3 bp and 3 aa substitutions). In all 3 tumors, there was evidence of B cells actively undergoing somatic hypermutation, as numerous sequences were identified with identical VDJ junctions but distinct mutation patterns. Thus, as hypothesized, TIL-B show strong evidence of antigen recognition.

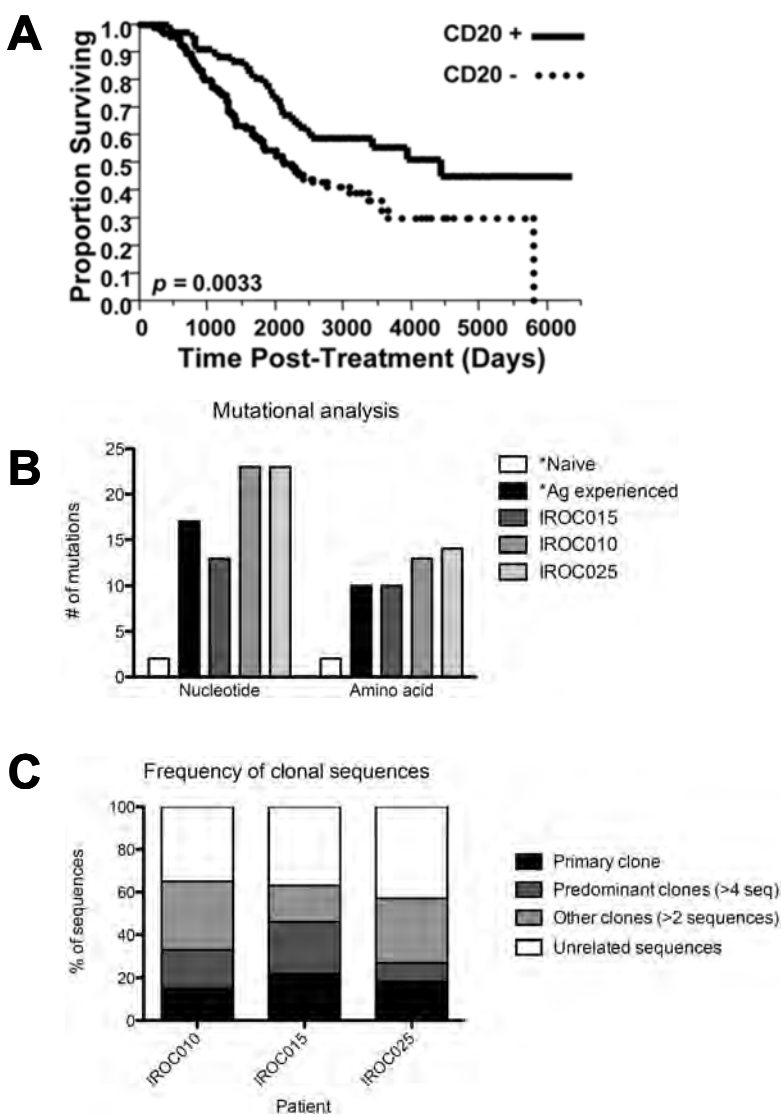


Figure 2. Tumor-infiltrating B cells (TIL-B) are associated with survival in ovarian cancer, and show evidence of antigen recognition. **(A)** Kaplan-Meier analysis showing that patients whose tumors contain CD20+ TIL-B have significantly increased survival (from Milne et al. 2009, PLoS One). **(B,C)** Sequencing of IgG molecules from three ovarian cancer patients (IROC015, IROC010 and IROC025) reveals evidence of **(B)** somatic hypermutation and **(C)** clonal expansion in 3/3 patients.

on these findings, we hypothesize that TIL-B might promote patient survival by processing and presenting tumor-specific antigens to CD4+ and CD8+ T cells in the tumor environment, thereby amplifying and sustaining anti-tumor responses. Over the next 1-2 years, we will investigate this hypothesis by (a) cloning IgG heavy and light chains from individual TIL-B (isolated by flow cytometry); (b) combining the heavy and light chains in a vector to produce single-chain recombinant IgG; and (c) using recombinant IgG to identify the corresponding tumor antigens by screening cDNA libraries and/or immunoprecipitating antigens from tumor

Second, we used the IgG sequencing data to estimate the extent of clonality of TIL-B by calculating the prevalence of each variable gene sequence in the dataset. Sequences were defined as clonal if at least two independent plasmids contained identical VDJ junctions. Variable region sequences that differed by just a single nucleotide were excluded, as these could potentially represent PCR artefacts. Using these criteria, we found evidence for at least 12-14 TIL-B clones in each tumor, some of which were highly represented. For example, in IROC015, 16% of sequences were derived from a single TIL-B clone, an additional 17% of sequences were derived from 2 other predominant clones, a further 36% of sequences were derived from 9 minor clones, and the remaining 31% of sequences were unrelated (Fig. 2C). These trends were very similar across all 3 patients (Fig. 2C), indicating that TIL-B in general represent oligoclonal populations. We are currently preparing these results for publication.

In summary, TIL-B (a) are strongly associated with patient survival; and (b) show all the hallmarks of having undergone proliferation and differentiation in response to antigen recognition. Based

lysates followed by mass spectrometry. Once the antigens are identified, in Task 5 we will test whether these antigens are recognized by tumor-infiltrating T cells from the same patients (as per our original proposal). If so, this will accomplish the major goal of this project: to identify the antigens recognized by tumor-infiltrating T cells. It will also provide strong support for the hypothesis that TIL-B serve as antigen presenting cells in the tumor environment. Such a finding would have very important implications for the future immunotherapy of ovarian cancer, as it would suggest that it would be beneficial to induce both T cell and B cell responses in patients to elicit potent, sustained anti-tumor immunity.

Task 4. To identify changes to the tumor transcriptome induced by chemotherapy in EOC.

In a parallel approach aimed at identifying tumor antigens, we proposed to subject primary and recurrent tumor cells to whole-transcriptome cDNA sequencing using a massively parallel sequencing platform (Illumina). Data would then be analyzed to identify sequence alterations or changes in expression level that differ between primary and recurrent tumor tissue using constitutional DNA from matched PBMC as a reference. We expect to identify sequence alterations arising in recurrent tumor cells, including point mutations, deletions and rearrangements. Potential CD8+ T cell epitopes would be identified using computer algorithms predictive of MHC binding.

Progress to date: Mutational profiling of the protein-coding regions of the genome (referred to as the “exome”) has begun for three patients (IROC02, IROC12 and IROC24). As proposed, we focused on CD45-negative tumor cells sorted from ascites samples collected (a) prior to treatment, and (b) upon first and second recurrence. To sequence the whole tumor exome, genomic DNA was isolated from CD45- cells and used to construct Illumina sequencing libraries. Peripheral blood mononuclear cells (PBMCs) from pretreatment blood draws from the same patients served as a source of normal germline DNA. Exon-encoding sequences were enriched by hybridization to exon probes, followed by massively parallel sequencing on the Illumina platform.

Specimens from IROC024 were sequenced first. Libraries derived from primary, recurrent and normal specimens were sequenced on a single lane of an Illumina flowcell, which generated over 70 million reads of 75 bp in length (Table 1). Uniquely aligned reads accounted for over 50 million of the reads, and the number of nucleotides that were available for variant detection numbered in the billions. Single nucleotide variant (SNV) analysis was performed on these first three libraries by using a multi-tiered, bioinformatic approach to variant calling.

Table 1: Summary of sequence library coverage and SNVMix variant calling.

Sample	Matched Normal	Primary tumor	Recurrent tumor
Library ID	HS2864	HS2863	HS2435
Flow cell ID	62JNFAAXX_6	62JNFAAXX_5	61YE4AAXX_7
Total number of reads	82,101,194	79,682,670	70,816,890
Number of unique read alignments	62,275,234	61,388,837	54,258,832
Number of reads used for SNVMix	28,251,373	43,509,439	29,337,411
Number of bases used for SNVMix	2,113,779,103	3,256,685,791	2,191,292,449
Number SNVMix variants	625	690	542
Number SNVMix synonymous variants	223	235	194
Number SNVMix non-synonymous variants	402	455	348

The first tier of SNV calling was determined by the program, SNVMix, which identified over 500 SNVs in the exomes of each of the libraries. The SNVMix variants were entered into a

MySQL database so that germline SNVs from the normal library could be subtracted from the tumor libraries and comparisons between primary and recurrent tumor libraries could be made. This revealed 99 non-synonymous coding SNVs that were specific to primary tumor cells, 39 coding SNVs specific to recurrent tumor cells, and 44 coding SNVs that are shared by both (Fig. 3). The second tier of SNV calling involved cross referencing the SNVMix variants to SNVs identified by another bioinformatic program called Samtools, which reduced the number of putative mutations by about half. The final tier of calling SNVs is currently underway using a program called TASR, a stringent, short-read assembling program. Putative mutations that pass all three tiers of bioinformatic analysis will be validated by PCR amplification followed by Sanger sequencing. Furthermore, samples from two additional patients (IROC002 and IROC012) have been submitted for sequencing on the Illumina platform, and we expect to receive the raw sequencing data by the end of April 2011. This data will be analyzed using the above bioinformatic methods.

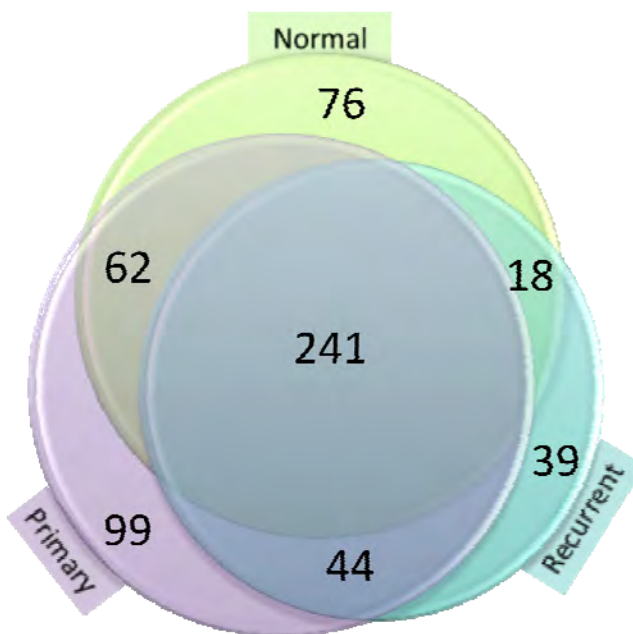


Figure 3: Variant relationships between normal cells, primary tumour cells and recurrent tumour cells. Ascites from patient IROC024 was collected and sorted for sequencing the whole exomes of CD45+ normal cells taken prior to treatment, CD45-primary tumor cells taken prior to treatment and CD45- recurrent tumor cells taken after one round of treatment. Single nucleotide variants (SNVs) were called by the program SNVMix and the novel non-synonymous coding SNVs were compared between libraries.

Task 5. To determine whether tumor-associated CD8+ T cells in EOC recognize putative chemotherapy-induced antigens.

We proposed to use Interferon- γ ELISPOT to test candidate antigens from Tasks 3 and 4 for recognition by CD8+ T cells from recurrent ascites. RNA-transfected or peptide-pulsed

CD40L-stimulated B cells would serve as antigen presenting cells. The clinical time point at which antigen-specific T cell responses arise would be assessed by ELISPOT analysis of serial blood samples and primary vs. recurrent ascites samples.

Progress to date: This aim depends on the results of Tasks 3 and 4, therefore it is not expected to commence for 3-6 months. Nonetheless, we have been developing our ELISPOT platform in preparation for this work. Specifically, we have optimized methods for performing *in vitro* stimulation and expansion of antigen-specific human CD8+ T cells. For this purpose, we have used the melanoma tumor antigen MART-1, which is often used as a model antigen for tumor immunology studies. As described in our 2010 report, our methods are optimized to the point where we can activate and expand naive MART-1-specific CD8+ T cells reliably from normal donors. We also developed and published a new method for multiplexed analysis of antigens using tandem mini-genes encoded by *in vitro* transcribed RNA (Nielsen et al., *J. Immunological Methods*, 2010; **APPENDIX C**). Thus, we are now prepared to analyze novel tumor antigens as they arise from Tasks 3 and 4. We expect to begin this analysis in Q3/Q4 of 2010, after the sequencing data from Task 4 has been fully validated, and tumor-specific mutations are in hand for the first three patients (IROC002, IROC012, and IROC024).

KEY RESEARCH ACCOMPLISHMENTS:

- Task 1: Specimen collection is proceeding as planned. We have been successful at collecting matched primary and recurrent tumor samples from 12 patients (**Fig. 1**). However, only one patient has met the 24 month PFI criteria so far; 12 other patients are candidates to meet this criterion.
- Task 1: We have optimized flow cytometric methods for isolating tumor cells and T cells for massively parallel sequencing.
- Task 2: We have further optimized our innovative method for analyzing the human T cell repertoire using massively parallel sequencing (Warren et al., *Genome Research*, 2011; **APPENDIX A**).
- Task 2: We have identified unique T cell clonotypes in recurrent ascites from one patient. We will proceed to profile the T cell repertoire at greater depth using our innovative deep sequencing approach.
- Task 2: We have developed methods using multiparameter flow cytometry to analyze the functional properties of tumor-reactive CD4+ and CD8+ T cells in the tumor environment (Tran et al. *PLoS One*, 2010).
- Task 3: We have shown that tumor-infiltrating B cells (TIL-B) are strongly associated with survival in ovarian cancer (**Fig. 2A**), and the PI wrote a review article discussing this issue (Nelson, *J. Immunology*, 2010; **APPENDIX B**). Based on this new appreciation for the prognostic significance of TIL-B, we have modified our autoantibody-based antigen identification strategy to use IgG derived from TIL-B (**Fig. 2B,C**), rather than serum IgG.
- Task 4: We have optimized methods for whole exome sequencing, a method that enriches for the protein-coding region of the genome.
- Task 4: Samples from the first patient (IROC024) have been analyzed by whole exome sequencing; we have detected putative mutations at high stringency in the primary and recurrent tissue from this patient (**Fig. 3**).
- Task 4: Samples from two more patients (IROC002 and IROC012) have been submitted for sequencing, and the raw data should be available in April 2011.

- Task 5: We optimized methods for in vitro expansion of human CD8+ T cells for ELISPOT.
- Task 5: We developed and published a new method for multiplexed analysis of antigens using tandem mini-genes encoded by *in vitro* transcribed RNA (Nielsen et al., *J. Immunological Methods*, 2010; **APPENDIX C**).

REPORTABLE OUTCOMES:**Relevant manuscripts published in 2010:**

1. Nelson BH. 2010. CD20+ B cells: the other tumor-infiltrating lymphocytes. *J Immunol.* 185(9):4977-82. Review. PMID: 20962266.
2. Nielsen JS, Wick DA, Tran E, Nelson BH, Webb JR. 2010. An in vitro-transcribed-mRNA polyepitope construct encoding 32 distinct HLA class I-restricted epitopes from CMV, EBV, and Influenza for use as a functional control in human immune monitoring studies. *J Immunol Methods.* 360(1-2):149-56. PMID: 20637775.
3. Tran, E., Nielsen, J.S., Wick, D.A., Ng, A.V., Nesslinger, N.J., McMurtrie, E., Webb, J.R., Nelson, B.H. 2010. Polyfunctional T-cell responses are disrupted by the ovarian cancer ascites environment and only partially restored by clinically relevant cytokines. *PLoS One.* 5(12):e15625. PMID: 21203522.
4. Warren RL and Holt RA. 2010. A census of predicted mutational epitopes for immunological cancer control. *Hum. Immunol.* 71(3):245-54.
5. Warren RL, Freeman JD, Zeng T, Choe G, Munro S, Moore R, Webb JR, Holt RA. Exhaustive T-cell repertoire sequencing of human peripheral blood samples reveals signatures of antigen selection and a directly measured repertoire size of at least 1 million clonotypes. *Genome Research.* Epub 2011 Feb 24.
6. Webb JR, Wick DA, Nielsen JS, Tran E, Milne K, McMurtrie E, Nelson BH. 2010. Profound elevation of CD8+ T cells expressing the intraepithelial lymphocyte marker CD103 (alphaE/beta7 Integrin) in high-grade serous ovarian cancer. *Gynecol Oncol.* 118(3):228-36. PMID: 20541243.

Leveraged funding:

We have active funding for the following projects related to this DOD project:

1. Canadian Institutes of Health Research (CIHR) – Grant#:MOP97897

10/2009 – 09/2012

Tumor-infiltrating T cells in ovarian cancer: functional impact on patient survival

Goal: To define the functional phenotype of tumor-infiltrating T cells in ovarian cancer.

PI: Brad Nelson

Co-PI's: John Webb, Peter Watson, Julian Lum

2. Canadian Institutes of Health Research (CIHR) - Grant#: MOP-102679

04/2010 – 03/2014

Characterizing the human T-cell receptor repertoire by massively parallel sequencing

Goal: To characterize individual variation in the human T-cell repertoires at sequence level resolution, using a comparative approach.

PI: Rob Holt

Co-PI: John Webb

CONCLUSION:

Overall, this study is progressing on schedule and on budget, with no major deviations from the original proposal. We are going through the anticipated waiting period associated with the collection of recurrent tumor specimens from patients experiencing a favorable progression-free interval. In the meantime, we have optimized methods for cell sorting of tumor cells, whole exome sequencing, and in vitro expansion of human T cells for ELISPOT. We published 6 relevant manuscripts in 2010. Additional funding has been received from several other agencies, enhancing the strength of our ovarian cancer research program.

REFERENCES:

None.

APPENDICES:

- A. Warren RL, Freeman JD, Zeng T, Choe G, Munro S, Moore R, Webb JR, Holt RA. Exhaustive T-cell repertoire sequencing of human peripheral blood samples reveals signatures of antigen selection and a directly measured repertoire size of at least 1 million clonotypes. *Genome Research*. Epub 2011 Feb 24. PMID: 21349924.
- B. Nelson BH. 2010. CD20+ B cells: the other tumor-infiltrating lymphocytes. *J. Immunol.* 185(9):4977-82. Review. PMID: 20962266.
- C. Nielsen JS, Wick DA, Tran E, Nelson BH, Webb JR. 2010. An in vitro-transcribed-mRNA polyepitope construct encoding 32 distinct HLA class I-restricted epitopes from CMV, EBV, and Influenza for use as a functional control in human immune monitoring studies. *J. Immunol. Methods*. 360(1-2):149-56. PMID: 20637775.

SUPPORTING DATA:

None.

Resource

Exhaustive T-cell repertoire sequencing of human peripheral blood samples reveals signatures of antigen selection and a directly measured repertoire size of at least 1 million clonotypes

René L. Warren,¹ J. Douglas Freeman,¹ Thomas Zeng,¹ Gina Choe,¹ Sarah Munro,¹ Richard Moore,¹ John R. Webb,² and Robert A. Holt^{1,3,4}

¹BC Cancer Agency, Michael Smith Genome Sciences Centre, Vancouver, British Columbia V5Z 1L3, Canada; ²BC Cancer Agency, Deeley Research Centre, Victoria, British Columbia V8R 6V5, Canada; ³Department of Molecular Biology and Biochemistry, Simon Fraser University, Burnaby, British Columbia V5A 1S6, Canada

Massively parallel sequencing offers a useful approach to characterizing TCR diversity. However, immune receptors are extraordinarily difficult sequencing targets because any given receptor variant may be present in very low abundance and may differ legitimately by only a single nucleotide. As such, the sensitivity of sequence-based repertoire profiling is limited by both sequencing depth and sequencing accuracy. We obtained peripheral blood TCRB mRNA from a healthy donor, at two timepoints 1 wk apart, and generated from multiple libraries a total of 1.7 billion paired sequence reads. The sequencing error rate was determined empirically, by analyzing the portion of each read encoding one of a small number of possible J segments, and used to inform a high stringency data filtering procedure. From the error filtered data, we obtained 1,061,522 distinct TCRB nucleotide sequences. This figure establishes a new, directly measured lower limit on individual T-cell repertoire size and provides a useful reference set of sequences for repertoire analysis. Analysis of naïve (CD45RA+/CD45RO-) and memory (CD45RA-CD45RO+) T-cell fractions highlighted T-cell plasticity, whereby sequences that were highly represented in both subsets at week 1 had transitioned preferentially to the CD45RA-/CD45RO+ subset at week 2. TCRB nucleotide sequences obtained from two additional donors were compared with those from the first donor and revealed highly similar V and J gene usage frequencies among individuals, but only a very small proportion (<1.1%) of shared nucleotide sequences. Analysis of in silico translated sequences indicated, however, that at the amino acid level as many as 14.2% of distinct sequences from one donor were shared with those from another donor. For each donor, shared amino acid sequences were encoded by a much larger diversity of nucleotide sequences than were unshared amino acid sequences. We also observed a highly statistically significant association between numbers of shared sequences and shared HLA class I alleles.

[Supplemental material is available for this article. The sequencing data from this study have been submitted to the NCBI Sequence Read Archive (<http://www.ncbi.nlm.nih.gov/Traces/sra/sra.cgi>) under accession no. SRA020989. A file containing all distinct TCRB sequences observed after all quality filtering is available at <ftp://ftp.bcgsc.ca/supplementary/TCRb2010/>.]

T lymphocytes are key mediators of adaptive immunity that recognize heterologous cells expressing foreign or mutated proteins. Recognition is mediated by the interaction of cell surface molecules, whereby a heterodimeric T-cell receptor (TCR) on the surface of a T lymphocyte will bind to a protein degradation product from the heterologous cell that is presented at the surface of that cell by the major histocompatibility complex (MHC). To generate a repertoire of structurally variant TCRs capable of recognizing diverse peptide-MHC (pMHC) complexes, the locus encoding the receptor undergoes somatic recombination among the Variable (V), Diversity (D), and Joining (J) gene segments, plus the addition/subtraction of nontemplated bases at recombination junctions (Davis and Bjorkman 1988; Bassing et al. 2002). The process is directly anal-

ogous to the generation of antibody diversity by somatic VDJ recombination of the B-cell receptor locus. Like antibody diversity, the potential for TCR diversity is nearly infinite, but actual diversity in a biological repertoire is restricted by deletion of over- and under-reactive cells during thymic maturation and is molded continuously by the clonal expansion of antigen responsive cells in the periphery (Nikolich-Zugich et al. 2004; Harty and Badovinac 2008).

By allelic exclusion, a T cell typically expresses only a single TCRB variant (Khor and Sleckman 2002), making beta-chain sequence variation a useful measure of T-cell repertoire diversity. The vast majority of TCRB variation is within the CDR3 (Complementary Determining Region 3), which encompasses the VDJ recombination junctions and encodes the portion of the TCR that directly contacts pMHC (Davis and Bjorkman 1988). We use the sequence of the CDR3 plus the identity of the flanking V and J gene segments to uniquely classify TCRB variants.

Sequence diversity in both T-cell and B-cell immune repertoires has been surveyed previously (Boyd et al. 2009; Freeman et al. 2009;

⁴Corresponding author.
E-mail rholt@bcgsc.ca

Article published online before print. Article, supplemental material, and publication date are at <http://www.genome.org/cgi/doi/10.1101/gr.115428.110>. Freely available online through the *Genome Research* Open Access option.

Robins et al. 2009; Klarenbeek et al. 2010; Wang et al. 2010) but not exhaustively sequenced. Here, we analyze TCR beta-chain sequences from peripheral blood from a single healthy individual, and we compare this immune repertoire to survey sequence from two other healthy individuals. We find that by exhaustive sequencing and careful mitigation of sequencing error, it is possible to saturate the diversity within a single sequencing library and within a sample of peripheral blood. However, determining the true size of an immune repertoire by exhaustive sequencing is intractable because a repertoire can only be subsampled, and by the nature of “next-generation” sequencing technologies where sequencing errors are incurred at a constant rate, it is not possible to distinguish very rare sequences from sequencing errors. Still, immune repertoire analysis by massively parallel sequencing offers tremendous utility, where distinct clonotypes can be readily identified and tracked, diversity can be profiled, and differences among individuals or subsets of sorted cells can be readily distinguished. All data from the present study have been made available as a community resource to facilitate future comparative studies of immune repertoires.

Results

With informed consent, we isolated PBMCs (peripheral blood mononuclear cells) from 20 mL of peripheral blood samples. These samples were obtained at two timepoints, 1 wk apart, from unrelated Caucasian donors (age 29–33 yr) with no self-declared immune-related disorder. Total RNA was isolated from ficoll-purified PBMCs and reverse transcribed using a 3' primer specific for the two conserved TCR beta-chain C genes. A 5' priming site was added to cDNA molecules during reverse transcription by template switching (Peters et al. 1999). The TCRB sequence was then amplified by PCR and directionally sheared to remove uninformative V gene nucleotides, leaving the distal part of the V gene, the informative CDR3 sequence, and the J segment (TRBJ) intact. This procedure shortened templates to ~130–180 bp, a length appropriate for Illumina library construction and paired-end sequencing, and allowed double-strand coverage of the critical CDR3 region.

Recognition and mitigation of sequence error is essential for accurate repertoire enumeration

Immune receptors are extraordinarily difficult sequencing targets because any given receptor variant may be present in very low abundance and may differ legitimately from other receptor variants by only a single nucleotide. The first PBMC sample from the first donor, a healthy 29-yr-old male, contained ~12 million $\alpha\beta$ T-cells. By using standard procedures, we constructed an Illumina sequencing library from the shortened 5'-RACE products from this first donor and ran six lanes of Illumina GAIx sequence to obtain 142.1 million pairs of reads. To assess sequence accuracy, we aligned raw reads to the known TCR J gene segments, of which there are 13 annotated in the human genome (Flück et al. 2010). From aligned raw single pass reads, we observed 9.4 errors per kilobase, but when we added the requirements of (1) double-strand coverage, (2) minimum quality score (Ewing and Green 1998) of Q30, and (3) no high-quality discrepancy between strands at any position, the error rate fell to 2.2 errors per kilobase. However, when we realigned the quality-filtered data to the 13 reference J gene segments, this residual sequence error still generated thousands of distinct J genes (Fig. 1A). The presence of a huge excess of distinct sequences that are

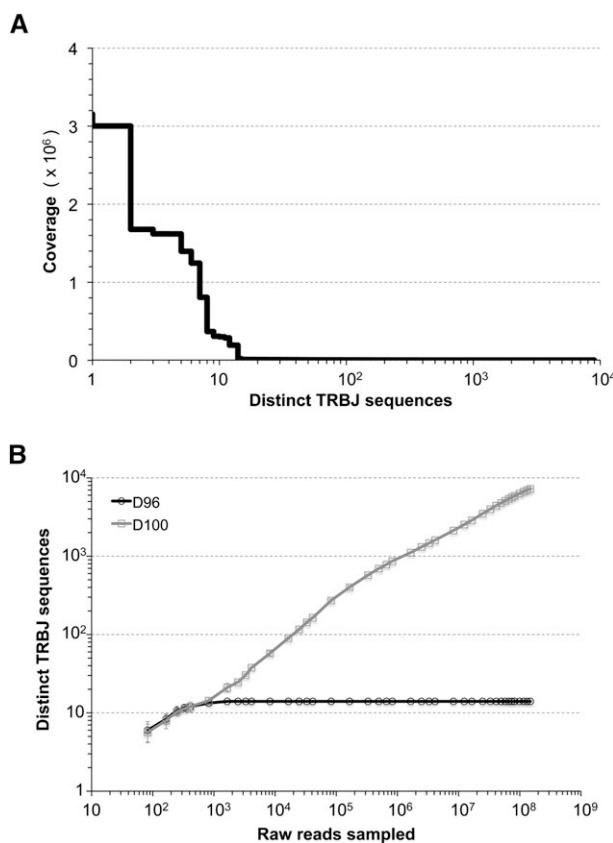


Figure 1. Distinct TCRB sequences. (A) Sequence coverage of distinct TRBJ sequences observed upon alignment of Illumina reads quality filtered to >99.9% predicted accuracy (Q30). There was substantial coverage, up to several million-fold, of the 13 human TRBJ segments, but thousands of artificial distinct TRBJ sequences were also observed, arising from residual sequencing error. (B) Restricting the data set to D96 effectively retains all real TRBJ sequences and excludes all of the artificial TRBJ sequences observed when no coverage restriction is applied (D100).

artifacts is clearly problematic when the goal is to enumerate the number of real distinct sequences in a sample. We found that even more aggressive quality filtering (i.e., a higher Q value threshold) was not helpful and that redundancy was the only useful metric for distinguishing real from erroneous sequences. We observed that the 13 J segments were represented by 96% of the data, with 1.1 ± 0.9 (mean \pm SD) million-fold coverage, and the remaining 4% of the data represented all of the thousands of artificial J sequences, with 78 ± 448 (mean \pm SD)-fold coverage. Thus, by restricting the data set to those distinct sequences that are represented by 96% of the data, all real sequences were retained and all erroneous sequences were removed (Fig. 1B). We call this a D96 cutoff. A D50 cutoff, for example, would restrict the data set to fewer but higher copy number sequences, which together would account for 50% of the data and could not be artifacts because the same sequence errors could not, by chance, have been incurred at the same position so many times. A D100 data set would be unrestricted but highly error prone because it would contain many distinct sequences at low copy number, where sequences were grouped together because of the chance occurrence of the same sequencing error at the same position not because they represent the same T-cell clone. The corollary of this feature of the data is that it is not

possible to distinguish between sequences from very rare T cells and sequencing errors.

Having determined, empirically, that D96 is an appropriate cutoff for eliminating artifactual sequences, we applied the D96 restriction to CDR3, the highly variable region of TCRB that comprises the VDJ recombination junctions and for which no reference sequence exists. The error model and threshold derived from analysis of J sequence will be even more stringent when applied to CDR3 because CDR3 is located in the middle of the 5'-RACE amplicon, where double-stranded coverage and consensus quality are highest. We used the standard definition of CDR3 as the region between the last conserved cysteine of the V gene and the first conserved phenylalanine of the J gene in the conserved motif FGXG, and we defined a distinct TCRB sequence as having a precise VDJ rearrangement, effectively captured by the CDR3 sequence signature, flanking V and J genes, and deleted 3'V and 5'J bases. The D gene segment is too short to reliably annotate and is contained within CDR3 variation.

TCRB diversity is greater than that captured by a single library or a single blood sample

Quality filtering and D96 restriction of 142.1 million raw reads pairs obtained from the first library yielded 181,258 distinct TCRB sequences. Saturation analysis predicted that even deeper sequencing would not produce very many new sequences (Supplemental Fig. S1); however when we obtained an additional lane of Illumina data from a second library that had been constructed from the same blood sample, we observed, unexpectedly, that 74.8% of quality filtered TCRB sequences from this second library were novel. Library exhaustion is a recognized but under-reported phenomenon of massively parallel sequencing, and at least for the present application, our data clearly show that a single library may not adequately capture the diversity of a biological sample. Recognizing this limitation, we constructed 10 additional libraries, consuming all of the starting PBMC RNA from the first blood sample from this donor. We sequenced one to two lanes from each of the new libraries to obtain 632.7 million pairs of raw reads (Table 1). This is a large data set equivalent to about 50-fold coverage of the entire human genome. The data were quality filtered and D96 restricted as described above, yielding 494,796 distinct TCRB sequences, each with ninefold or higher coverage (Table 1).

We also sequenced five libraries constructed from a second 20 mL blood sample from the same subject 1 wk later (day 8), obtaining 149.5 million raw read pairs and 352,139 distinct TCRB

sequences (Table 1). We performed saturation analyses to determine how much of the diversity, within each blood sample, had been captured. By rarefaction analysis (random resampling of increasingly larger subsets of the data), there is an appearance of saturation sequencing of both blood samples (Fig. 2A) but a higher total number of distinct sequences obtained for blood draw 1, which was sequenced much deeper than blood draw 2. It is important to note, however, that rarefaction curves are not informative regarding total abundance and that by random resampling any data set will show a trend toward saturation. Therefore, in addition to rarefaction, we used accumulation analysis, whereby we plotted the number of distinct sequences found in each new library sequenced against the total number of distinct sequences from the blood sample as a whole. This approach, which takes into account the limitation of library exhaustion, illustrates that nearly all of the diversity present in the first blood sample has been captured (Fig. 2B). Interestingly, 33.5% of total sequences from the second blood sample were observed in the first, but after collapse into distinct sequences, there was only 12.8% overlap (Fig. 2C). This illustrates that independent blood samples contain many of the same abundant clonotypes but, due to the stochastic nature of sampling, fewer rare clonotypes. Further, it illustrates that a 20 mL blood sample captures only a portion of the diversity present within an individual's peripheral blood repertoire.

Diversity and plasticity of CD45RA⁺/RO[−] and CD45RA[−]/RO⁺ T-cell subsets

To compare diversity between naïve and memory T-cell subsets, we analyzed a separate 20 mL sample of peripheral blood from the same healthy 29-yr-old donor, taken on day 1. From this sample, we FACS sorted 1.3 million CD3⁺/CD45RA⁺/CD45RO[−] cells (naïve) and 1.0 million CD3⁺/CD45RA[−]/CD45RO⁺ cells (memory) (Supplemental Fig. S2). TCRB mRNA was amplified by 5'-RACE, Illumina sequenced, and quality filtered as described above to yield 55,253 and 52,166 distinct TCRB sequences, respectively (Table 1). We see very similar clonal diversity within these two T-cell subsets (Fig. 3A), with only slightly higher clonality detected within the memory subset. Surprisingly, we found that only a portion of sequences from the naïve and memory subsets matched sequences obtained from the deep analysis of unsorted cells from this donor (Fig. 3B). This is likely due to the fact that the cells are from an independent blood draw, and therefore, sequence signatures would be expected to overlap only partially. Very few (<1% for naïve and <3% for memory) of the new sequences found within the sorted subsets matched anything that had been removed by D96 restriction from the deep sequencing

Table 1. TCRB sequence statistics

Subject	Timepoint ^a	Cell type	T-cell content (×10 ⁶)	No. of libraries	Raw reads sequenced	D96 cutoff	Total TCRB sequences (nt)	Distinct TCRB sequences (nt)	Productive rearrangements ^b (%)
Male 1	Day 1	PBMC	12.0	11	1,265,489,402	9	188,287,192	494,796	99.0
	Day 8	PBMC	13.2	5	299,077,972	3	21,383,933	352,139	98.8
	Day 1	RO ⁺ /RA [−]	1.0	1	38,069,567	44	15,559,088	52,166	98.5
	Day 1	RA ⁺ /RO [−]	1.3	1	37,764,624	19	14,754,019	55,253	98.2
	Day 8	RO ⁺ /RA [−]	0.7	1	29,199,761	5	15,615,214	83,206	99.1
	Day 8	RA ⁺ /RO [−]	0.7	1	28,881,946	3	15,128,814	121,233	99.0
Male 2	Day 1,8	PBMC	16.4, 18.2	3	307,058,456	2	6,219,383	193,551	98.4
Female	Day 1,8	PBMC	18.2, 18.0	2	91,110,650	2	1,069,612	93,990	98.5

^aSame-day samples are independent blood draws.

^bTCRB sequence in correct reading frame that passed base quality filtering at the D96 cutoff.

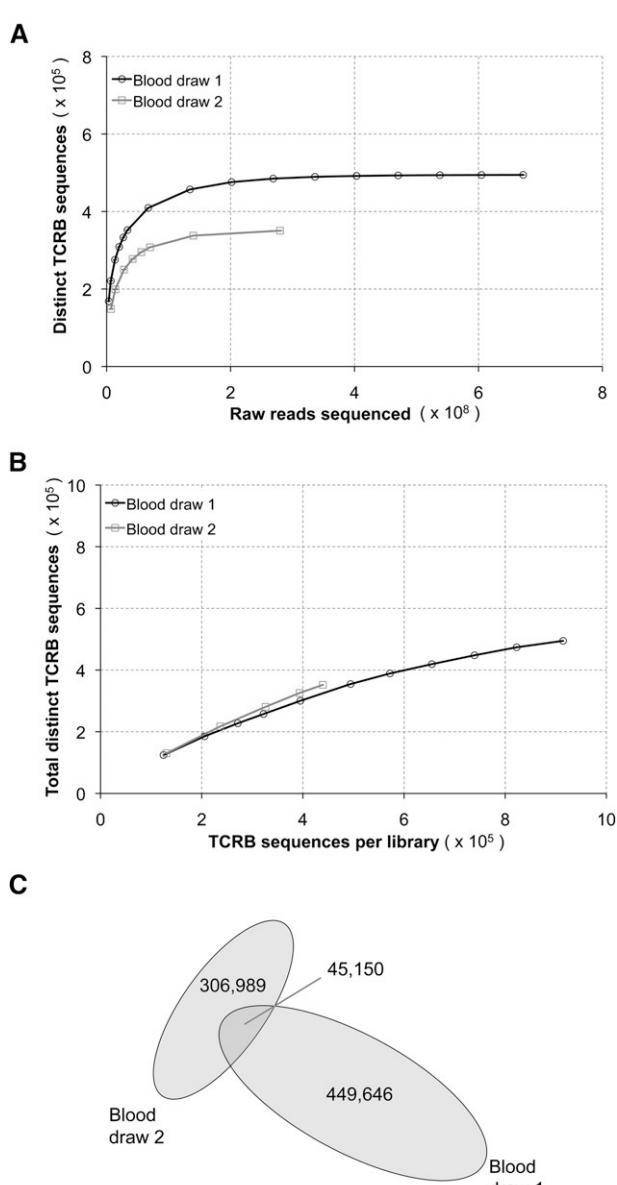


Figure 2. TCRB diversity in peripheral blood samples. (A) Rarefaction curves plotted using all data from all libraries from blood draw 1 (round symbols) and blood draw 2, taken 1 wk later (square symbols) from donor 1. Random resampling was done in triplicate, and error bars are contained within symbols. Both curves plateau, suggesting that more sequencing of either sample would not be expected to produce many new sequences. However, this tendency toward leveling is a property of rarefaction curves, and the plateau is not informative regarding absolute abundance. Hence, rarefaction curves must be interpreted with caution. (B) Accumulation analysis provides a more meaningful measure of saturation. Here we show the number of new distinct sequences found in each library (x-axis) against the total number of distinct sequences from the blood sample as a whole. The TCRB diversity within blood draw 1 from donor 1 appears to have been captured, since analyzing additional libraries would not be expected to yield many new TCRB sequences. In contrast to the rarefaction curve present in the previous panel, library-based accumulation shows that the diversity of blood draw 2 is similar to that of blood draw 1 but has not yet been fully captured. (C) Despite saturation of blood draw 1, sequences found in blood draw 2 only partially overlap, indicating that there is considerable un-sampled diversity within the peripheral blood TCRB repertoire of this individual.

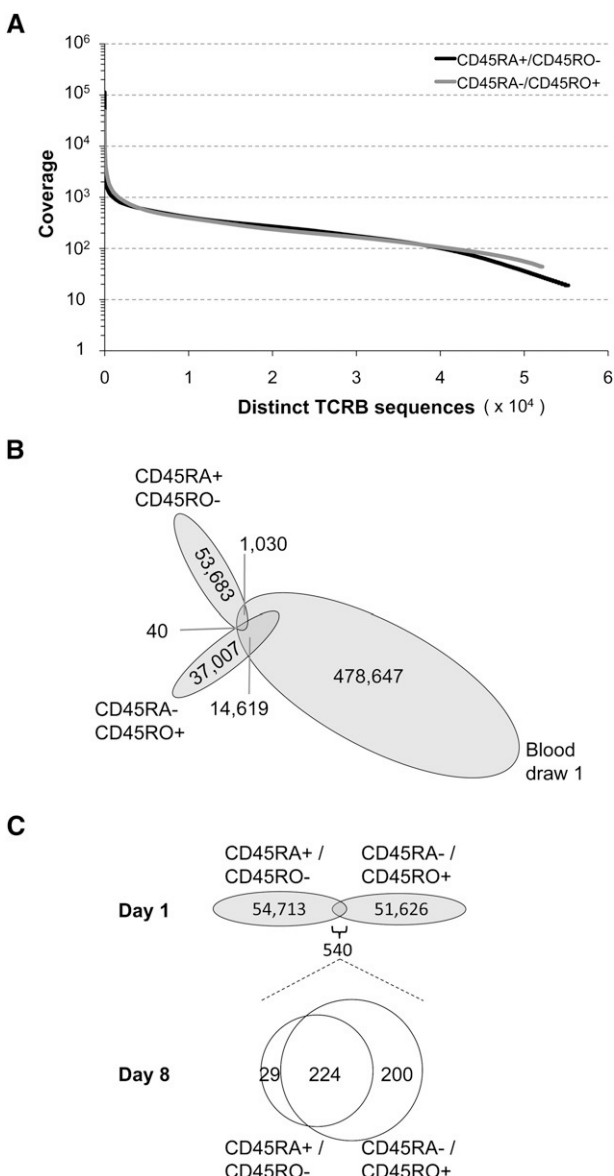


Figure 3. TCRB sequence diversity in the naïve and memory compartments of a deeply sequenced individual. (A) Frequency distributions of CD45RA+/CD45RO- (naïve) and CD45RA-/CD45RO+ (memory) T-cell subsets isolated by FACS from PBMCs from a separate blood sample from donor 1, taken on day 1. The similarity of the two curves reflects the presence of high diversity within both subsets, although this is slightly greater for the naïve subset, as evident from the extended tail of the distribution. There are, in both cases, a small number of extreme copy clonotypes and a relative clonotype abundance varying over four orders of magnitude. (B) There is more overlap with the deeply sequenced sorted cells for the memory versus the naïve subset, but even the overlap of the memory subset is modest. This is consistent with a large total repertoire size that can be only partially captured in a given blood draw. (C) Of the sequences that were shared between sorted naïve and memory cells on day 1, there was a preferential transition to the memory subset on day 8.

of PBMC-derived amplicons, so it is not the case that there was overly aggressive filtering of the deeply sequenced set.

We also observed 540 TCRB sequences, most having a high copy number, which were present in both populations of sorted cells (Supplemental Fig. S3). The observation of dual marker cells is

consistent with previous reports (Deans et al. 1989; Johannisson and Festin 1995, Wang et al. 2010). Because sorted cells were of high purity (Supplemental Fig. S2), it is unlikely that this mixed phenotype is an artifact of sorting. Rather, these cells may represent a population of acutely expanded effectors where the expression of CD45RA+ versus CD45RO+ is in transition. To address this question, we sorted cells from an additional sample of peripheral blood from this donor, taken on day 8, into CD3+/CD45RA+/CD45RO- and CD3+/CD45RA-/CD45RO+ subsets, and sequenced and analyzed as above (Table 1). Of the 540 TCRB sequences that were shared between the memory and naïve compartment on day 1, 453 were re-identified on day 8. Of these, 224 were still found in both populations of sorted cells. However, of those that were found at day 8 in only one cell population or the other, 29 were in the CD45RA+ population and 200 were in the CD45RO+ population. This illustrates plasticity of a T-cell subset, as defined by surface marker expression, and a preferred directionality for transition (Fig. 3C).

A modest proportion of sequences are shared among individuals, and these show a signature of antigen selection

To compare repertoire diversity among the individuals, we obtained, with informed consent, peripheral blood samples (20 mL) from two additional healthy, unrelated donors. One of the new donors (male, 33 yr) had no HLA class I match to the first donor, and the other new donor (female, 33 yr) was matched to the first donor at all three HLA class I loci (Table 2). Two blood samples, taken 1 wk apart, were obtained from each donor, and these contained between 16.4 million and 18.2 million $\alpha\beta$ T-cells. PBMCs were purified, and TCRB sequencing was performed as described above to yield 193,551 and 93,990 distinct TCRB nucleotide sequences from each donor, respectively (Table 1). Due to the lower depth of sequencing, data from each of the two samples from the same donor were pooled. We determined the number of TCRB sequences from each of the two additional donors that were observed in any of the sample from the first donor. Doing the comparisons in this manner controls for the different sequencing depths achieved. Each repertoire was found to be mostly unique at the nucleotide level. The female donor shared 1.1% of her sampled TCRB sequences with male donor 1, and male donor 2 shared 0.7% of his sampled TCRB sequences with male donor 1. Next, we translated CDR3 sequences in silico and repeated this analysis, with markedly different results (Table 3). At the amino acid level, the female donor shared 14.2% of her sampled sequences with male donor 1, and male donor 2 shared 11.7% of his sequences with male donor 1. This is consistent with the notion that the response to antigen led to retention of certain preferred amino acid sequences that, due to degeneracy of the genetic code, were specified by a larger diversity of nucleotide sequences. The different nucleotide se-

quences would be expected to be contributed by different cells, such that in some cases a given T-cell specificity may represent responses from multiple, independent precursor cells. We then segregated sequences into those that were shared versus unique for a given donor. When the ratios of amino acid versus nucleotide sequences in these two groups were compared, the shared sequences have a much stronger signature of selection (Table 3). We observe a strong association between the sharing of HLA class I alleles and the proportion of shared TCRB sequences ($P < 1 \times 10^{-6}$, χ^2 test for two proportions), and we note that compared with unique sequences, shared sequences have shorter mean CDR3 length and higher mean abundance ($P < 1 \times 10^{-4}$, unpaired *t*-test or one-way ANOVA with Newman-Keuls post hoc test) (Table 3). Finally, in contrast to the predominant individuality of sequence specificity within repertoires, we observed striking similarity in the pairing frequency between the specific V and J gene segments among individuals (Supplemental Fig. S4). Pairwise comparisons between donors of V and J usage produced Pearson correlation coefficients of 0.87 ± 0.02 (mean \pm SD) and 0.79 ± 0.12 (mean \pm SD), respectively.

Discussion

Here we report the deepest sequencing of any immune repertoire to date, capturing a total of 1,061,522 TCRB sequences from a single individual. This value places a new lower boundary on T-cell peripheral repertoire size that is consistent with the long-standing estimate of approximately 1 million distinct TCRB sequences in peripheral blood (Arstila et al. 1999), which was derived by amplification and exhaustive sequencing of a small subset of specific V-J recombinants. However, the lower bound figure we report here is definitive because it is directly measured. We see only partial overlap between the two, independent, deeply sequenced blood samples from an individual (Fig. 2C), so it is clear that total peripheral blood repertoire size is higher still. In principle, it should be possible to estimate total repertoire size based on the observed overlap; however, the usual statistical methods, such as those used by ecologists to estimate species richness, are not well suited to this problem. They are confounded by the extreme heterogeneity in the abundance of different sequences observed within a library, the variation in sampling depth (i.e., number of sequence reads) among libraries, and the difficulty in distinguishing very rare sequences from sequencing errors. Thus, an accurate estimation of total repertoire size awaits the development of new statistical methods that can account for these issues.

For sequence-based repertoire profiling, the recognition and mitigation of sequencing error is extremely important. We show that even aggressive error filtering approaches that would be considered adequate for most applications are ineffective here, where there is very intensive sequencing of a short but highly variable target. The situation can be improved by using sequence redundancy as a metric for higher stringency error filtering. In our approach, co-amplified and sequenced J gene segments provide a useful empirical measure of error rate that can be used to inform quality filtering. We find that with appropriate error filtering, it is possible to exhaustively sequence a library and, by interrogating numerous libraries, exhaustively sequence a blood sample. Unethically intensive sampling would be necessary to exhaustively sequence a human immune repertoire.

In addition to measuring total TCRB diversity, we compared diversity within memory (CD45RA-/CD45RO+) and naïve (CD45RA+/CD45RO-) subsets. Following exposure to antigen, naïve cells proliferate rapidly and differentiate into effector cells.

Table 2. HLA class I alleles for TCRB repertoire profiling subjects

Subject	HLA class I Locus	Zygosity	Allele 1	Allele 2
Male 1	A	het	A*01:01P	A*25:01P
	B	het	B*08:01P	B*39:01P
	C	het	C*07:01P	C*12:03P
Male 2	A	het	A*02:01P	A*26:01P
	B	het	B*38:09	B*44:02P
	C	het	C*05:01P	C*12:03P
Female	A	homo	A*01:01P	NA
	B	homo	B*08:01P	NA
	C	homo	C*07:01P	NA

Table 3. Comparison of properties of shared and unique CDR3 sequences

	CDR3 (aa)	Depth (mean +/- SD)	Length (mean +/- SD)	CDR3 (nt) ^a	CDR3(aa) / CDR3(nt)
♀ total	86,255	12 +/- 309	13.89 +/- 1.57	89,663	0.96
♀ unique	73,006	10 +/- 52	14.02 +/- 1.59	73,947	0.99
♀ shared with ♂	13,249	24 +/- 779*	13.16 +/- 1.26*	15,716	0.84
♂ total	165,931	37 +/- 662	14.13 +/- 1.68	177,763	0.93
♂ unique	144,781	36 +/- 690	14.26 +/- 1.70	150,992	0.96
♂ shared with ♂	21,150	45 +/- 431	13.28 +/- 1.32*	26,771	0.79
♂ total	883,123	306 +/- 3844	14.55 +/- 1.72	1,004,790	0.88
♂ unique	852,181	292 +/- 3850	14.59 +/- 1.72	935,862	0.91
♂ shared with ♂	21,150	761 +/- 3036**	13.28 +/- 1.32**	50,649	0.42
♂ shared with ♀	13,249	851 +/- 4804**	13.16 +/- 1.26**	33,736	0.39

^aAn amino acid sequence can be encoded by more than one nucleotide sequence. CDR3(nt) refers to the total number of observed nucleotide sequences that encode the number of amino acid sequences specified in the adjacent column.

* $P < 0.0001$, comparison of shared and unique using an unpaired, two-tailed *t*-test.

** $P < 0.0001$, comparison of shared and unique using one-way ANOVA, Newman-Keuls post hoc test.

The splicing of the signaling molecule CD45 is altered so that the CD45RA+ isoform is replaced by the CD45RO+ isoform typical of effector and memory cells. While we were initially surprised to see comparable diversity in these two subsets, this observation is consistent with, and confirms, a recent report that both the CD45RA+ naïve subset and the CD45RO+ memory subset contain many unexpanded clones (Klarenbeek et al. 2010). The presence of abundant naïve (CD45RA+) clonotypes is puzzling as it is unclear why they would be expanded, if not in response to antigen exposure. It has been suggested, however, that these abundant CD45RA+ clonotypes may originate from proliferating cells that have not yet shifted to CD45RO+ expression or that there may exist populations of effector cells that have reverted to expression of CD45RA+ (Akondy et al. 2009). In our data from sorted cells, most TCRB sequences at day 1 are unique to one population, but there were hundreds of examples of an identical TCRB sequence being found in both the CD45RA+ and CD45RO+ sorted populations. At day 8, many more of these were found only in the CD45RO+ subset than were found only in the CD45RA+ subset (Fig. 3C). These results are consistent with a preferential transition to a memory phenotype, but interestingly, this is not absolute, since some cells did change to expressing CD45RA+ only.

By comparing TCRB nucleotide sequences sampled from two additional subjects to the deeply sequenced repertoire from the first subject, we see that sharing among subjects is minimal and that at the nucleotide level individual repertoires are largely distinct. The observation of any sequence sharing at all is remarkable, however, since the space of theoretically possible TCRB sequences is vast (Davis and Bjorkman 1988) and shared sequences would not be expected by chance. The observation of shared sequences has been reported recently (Robins et al. 2010), where it was noted that sharing was highly elevated compared to what would be expected by chance, when comparing to a model of total theoretical receptor diversity. Here, we confirm sequence sharing, and we show that sharing is much more extensive at the amino acid than at the nucleotide level. This is consistent with selective pressure on TCRs, whereby a TCR amino acid sequence with suitable antigen binding characteristics may be encoded, in

different cells, by different nucleotide sequences and selected independently.

One well-established mechanism of antigen selection is positive selection for HLA binding affinity during thymic T-cell maturation, and in our study, we see a clear association between proportions of shared TCR sequences and shared HLA class I alleles. Such an association has not been reported previously, and although ours is a preliminary observation based on only three subjects, it is highly statistically significant ($P < 1 \times 10^{-6}$). It suggests an influence of HLA type on T-cell repertoire features that deserves further scrutiny.

Methods

5'-RACE and preparation of 5'-RACE products for Illumina sequencing

Samples of peripheral blood (~20 mL each) were obtained by venipuncture. For

each of the three donors, samples were obtained on two separate days, 1 wk apart. PBMCs were isolated immediately from each sample by Ficoll-Paque (GE Healthcare) gradient centrifugation. For male donor 1, an additional, independent blood sample was taken on each day for the purpose of sorting the CD45RA+ and CD45RO+ subsets. To estimate numbers of T-cells in each sample, bulk PBMCs were stained with FITC-conjugated anti-human TCR $\alpha\beta$ (clone T10B9.1A-31) and PE-Cy5-conjugated anti-human CD3 (clone UCHT-1; both from BD Biosciences) and were analyzed on a FACS Calibur, collecting a total of 50,000 events. For library construction, cells were centrifuged at 400g and resuspended in 2.4 mL buffer RLT (Qiagen), and 600 μ L aliquots were passed through a 27-gauge needle. Each aliquot was processed using an RNeasy Plus Mini column (Qiagen) according to the manufacturer's specifications. The eluates were pooled and the concentration determined using a NanoDrop ND-8000 spectrophotometer. First-strand cDNA was synthesized using a published *TRBC* primer (5'>CACGTGGTCGG GGWAGAAGC<3') (Ozawa et al. 2008). A target-switching oligo (Peters et al. 1999) (5'>AAGCAGTGGTAAACACGCAGAGTACGC GGG<3') was added to provide a 5' template for RACE. First-strand synthesis reaction conditions were as follows: 333 ng RNA, oligonucleotides 1 μ M each, 2 mM DTT, 1 mM each dNTP, 50 mM Tris-HCl (pH 8.3), 75 mM KCl, 6 mM MgCl₂, 40 U of RNaseOUT (Invitrogen), and 200 U SMARTScribe Reverse Transcriptase (Clontech) in a 20 μ L volume. Extension was for 90 min at 42°C followed by inactivation for 15 min at 70°C. PCR was performed using Phusion Hot-Start DNA Polymerase (Finnzymes) and 8.0 μ L of first-strand reactions with long and short universal primers (5'>CTAATACGA CTCACTATAGGGCAAGCAGTGGTAAACACGCAGAGT<3' and 5'>CTAATCGACTCACTATAGGGC<3') and a nested *TRBC* primer, (5'>TCTCTGCTCTGATGGCTCAAAC<3'). Reaction conditions were as follows: 16 U enzyme, 1 \times Phusion HF amplification buffer, 3% DMSO, long universal primer at 0.1 μ M, short universal and nested primers at 0.5 μ M each, and 0.2 mM each dNTP in an 800 μ L volume. Each reaction was split into 50 μ L aliquots. For cycling, a 30-sec denaturation at 98°C was followed by 26 cycles of 10 sec at 98°C, 10 sec at 55°C, and 20 sec at 72°C, plus a final extension for 5 min at 72°C. The reaction was purified using two QIAquick columns (Qiagen), and the eluates were pooled and loaded on a 1.5% Tris-acetate low melting temperature agarose gel

(Seaplaque GTG, Mandel). The gel segment corresponding to a product size of 500–625 bp was excised and melted at 65°C in 1/10 volume of 3 M NaOAc, digested at 42°C with 1000U beta-Agarase (New England Biolabs) per milliliter for 2 h, and then purified by phenol extraction and ethanol precipitation. PCR was performed on a fraction of the first-round reaction with a nested universal primer (5'-ACGACTCACTATAAGGGCAAGCAG<3') and an equimolar combination of two biotinylated primers (5'-biotin/ACACT TAATTAACGGGTGGGAACACCTTGTTCAGGT<3') and (5'-biotin/ACACTTAATTAACGGGTGGGAACACGTTTCAGGT<3'), which contain 5' PacI sites and are specific for *TRBC1* and *TRBC2*, respectively. Reaction conditions were as follows: 800 ng purified fragment, 4 U Phusion Hot-Start DNA Polymerase (Finnzymes) 1× Phusion HF amplification buffer, 3% DMSO, 0.5 μM oligonucleotides, and 0.2 mM each dNTP in a 400 μL volume. A 30-sec denaturation at 98°C was followed by eight cycles of 30 sec at 98°C and 20 sec at 72°C, plus a final extension for 5 min at 72°C. The nested PCR reaction was purified using two QIAquick columns. Three micrograms was then sheared using the Covaris S1 (Applied Biosystems). Reaction conditions were as follows: 100 μL reaction volume, with a concentration of 100 ng/μL and 18 cycles with a duty cycle of 10%, intensity of 5, and cycles per burst at 200 for 30 sec. Biotinylated fragments were then purified using 100 μL of Dynabeads M-270 Streptavidin (Invitrogen) prepared according to the manufacturer's specifications. Washed and bound biotinylated fragments were then cleaved with PacI (reaction conditions; 1× NEB buffer 1, 100 μg/mL BSA, 50 U PacI [NEB] in a 300 mL volume for 2 h at 37°C followed by 20 min at 70°C) and ethanol precipitated.

The sample was loaded on a 8% polyacrylamide gel, and the fraction from 125–175 bp was excised, purified, and blunted. Reaction conditions were 1× NEB blunting buffer, 100 μM dNTPs, 1 μL blunting enzyme mix (NEB E1201S) in a 25 μL volume, for 30 min at 21°C. The product was purified by phenol/chloroform extraction and ethanol precipitation prior to A-tailing. Reaction conditions were as follows: 5 U Klenow fragment (3'→5' exo⁻; NEB), 1× reaction buffer, 200 μM dATP in a 50 μL volume, 30 min at 37°C. The product was purified by phenol/chloroform extraction and ethanol precipitation in preparation for ligation to Illumina PE adapters. Reaction conditions were as follows: 1× NEB T4 DNA ligase buffer, 1200 U T4 DNA ligase (NEB), 1 μL PE adapters in a 30 μL volume, 15 min at 21°C. The product was purified using a QIAquick column (Qiagen) and eluted in a volume of 30 μL. Ten microliters was then amplified by PCR using Illumina primers 1.0 and 2.0 (Reaction conditions; 1 U Phusion Hot-Start DNA Polymerase, 1× Phusion HF amplification buffer, 3% DMSO, 0.3 μM oligonucleotides, and 0.2 mM each dNTP in a 25 μL volume). A 2-min denaturation at 98°C was followed by 10 cycles of 10 sec at 98°C, 30 sec at 65°C, and 30 sec at 72°C, plus a final extension of 5 min at 72°C. The PCR product was purified using a MinElute column (Qiagen) with a final volume of 13 μL and further purified from a 8% polyacrylamide gel.

We chose to sequence mRNA, not the rearranged genomic locus, because VDJ rearrangement leaves residual and potentially interfering priming sites. For transcript sequencing, 5'-RACE is the method of choice because it mitigates the risk of PCR bias that could be incurred if amplification relied instead on using multiplexed V- and J-segment specific primers.

Illumina sequencing and analysis

Illumina libraries were sequenced (100- to 150-bp paired-end reads) using an Illumina GAIIX analyzer. Most data was of read length 114 bp, and sequencing to 150 bp did not increase substantially the yield of TCRB sequences post quality filtering. A microassembler

was developed to join overlapping paired-end reads from each sequencing template. Briefly, the assembler uses Exonrate (Slater and Birney 2005) to perform gapless alignments between any two mate pairs and joins the reads into sequence contigs, provided the reads align on opposite strands, facing inwards. Each alignment is scrutinized at run-time to resolve base conflicts, whenever applicable, and a consensus base sequence and quality score was generated for each newly formed contig. Agreeing bases on opposite strands were given a consensus score that corresponds to the sum of individual Q scores. Disagreeing bases were assigned an N at that position and a score of zero, unless the base call on one strand was 99.9% accurate or higher (\geq Q30) and the discrepant base on the other strand was <99% accurate (<Q20). In the latter case, the most accurate base was called. We found that 68.3% of all raw sequence pairs assemble and that attrition of pairs that do not assemble is due to many factors, including mixed clusters on the flow cell, sequence errors, and templates too long for mate pairs to overlap. Annotation of the aligned paired ends contigs was done as previously described (Freeman et al. 2009). Briefly, assembled pairs aligning to the 3' end of Ensembl *TRBV* gene predictions (Flicek et al. 2010) were retained and searched for the presence of 18 consecutive *TRBJ* segment bases. For any *TRBJ* segment, any 18-letter word from base positions 1–25 characterized uniquely that segment and allowed the identification of the precise *TRBJ* segment boundary as well as the number of *TRBJ* bases deleted. The *TRBV* segment boundaries and exact number of deleted *TRBV* bases were inferred by tracing back the alignments in the contig under scrutiny. Distinct TCRB sequences were identified as having unambiguous V and J segment annotation paired with a unique CDR3-encoded nucleotide sequence in a specific VDJ rearrangement that accounts for bases added and deleted at the junction. Only CDR3-encoded bases bearing no ambiguous (N) bases and having a base accuracy of 99.9% or higher at each base position were considered further. CDR3 is defined as the region between the last conserved cysteine of the V gene and the first conserved phenylalanine of the J gene in the conserved motif FGXG.

Real error rates were determined by analysis of *TRBJ* segments, which do not rearrange and for which reference sequences are known. This is important since the mechanism of base alteration within CDR3 that creates the vast diversity in T-cell specificity yields a sequence for which no reference exists. Errors were reported by comparing raw single-pass Illumina reads, double-strand coverage, and high-quality sequences to reference *TRBJ* sequences (Flicek et al. 2010). The latter set was further scrutinized to establish a sequence validity threshold by computing the proportion of J segments that did not match known *TRBJs* perfectly, as described in the Results section above.

HLA typing

HLA class I alleles were identified by sequence based typing. gDNA was extracted from patient granulocytes, and exons two and three from HLA class I genes (A, B, and Cw) were amplified by PCR using TAKARA polymerase (NEB), using primer sequences published previously (Cereb et al. 1995). PCR amplicons were inserted into a PCR-4-TOPO vector (Invitrogen) and cloned. Numerous clones for each locus were sequenced using an ABI 3730XL instrument according to standard procedures. Clone sequences were assembled using phred/phrap/Consed (<http://www.phrap.org>). The resulting sequence data were aligned against all available exon 2 and 3 nucleotide sequences from the 3.1.0 release of the IMGT/HLA database (Robinson et al. 2003) using ClustalW (Larkin et al. 2007). Allele assignments (four-digit codes) (Marsh et al. 2010) were based on high-quality exact or synonymous matches at informative nucleotide positions. Any PCR or cloning-based discrepancies were resolved manually, guided by

zygosity, proportional coverage, and the low likelihood that any low coverage sporadic variant represents a novel allele.

Acknowledgments

This work was funded by the Canadian Institutes of Health Research, Genome Canada, and Genome British Columbia. We thank Karen Lambie (BCCA) for assistance with phlebotomy, Winnie Sun (BCCA) for expert help with cell sorting, and Dr. Brad Nelson (BCCA) for helpful discussion of T-cell biology. We thank Carl Schwarz and Anne Chao for helpful discussion of statistical approaches to repertoire size estimation.

References

Akondy RS, Monson ND, Miller JD, Edupuganti S, Teuwen D, Wu H, Quyyumi F, Garg S, Altman JD, Del Rio C, et al. 2009. The yellow fever virus vaccine induces a broad and polyfunctional human memory CD8+ T cell response. *J Immunol* **183**: 7919–7930.

Arstila TP, Casrouge A, Baron V, Even J, Kanellopoulos J, Kourilsky P. 1999. A direct estimate of the human T cell receptor diversity. *Science* **286**: 958–961.

Bassing CH, Swat W, Alt FW. 2002. The mechanism and regulation of chromosomal V(D)J recombination. *Cell* **109**(Suppl): S45–S55.

Boyd SD, Marshall EL, Merker JD, Maniar JM, Zhang LN, Sahaf B, Jones CD, Simen BB, Hanczaruk B, Nguyen KD, et al. 2009. Measurement and clinical monitoring of human lymphocyte clonality by massively parallel VDJ pyrosequencing. *Sci Transl Med* **1**: 12ra23.

Cereb N, Maye P, Lee S, Kong Y, Yang SY. 1995. Locus-specific amplification of HLA class I genes from genomic DNA: Locus-specific sequences in the first and third introns of HLA-A, -B, and -C alleles. *Tissue Antigens* **45**: 1–11.

Davis MM, Bjorkman PJ. 1988. T-cell antigen receptor genes and T-cell recognition. *Nature* **334**: 395–402.

Deans JP, Boyd AW, Pilarski LM. 1989. Transitions from high to low molecular weight isoforms of CD45 (T200) involve rapid activation of alternate mRNA splicing and slow turnover of surface CD45R. *J Immunol* **143**: 1233–1238.

Ewing B, Green P. 1998. Base-calling of automated sequencer traces using phred. II. Error probabilities. *Genome Res* **8**: 186–194.

Flicek P, Aken BL, Ballester B, Beal K, Bragin E, Brent S, Chen Y, Clapham P, Coates G, Fairley S, et al. 2010. Ensembl's 10th year. *Nucleic Acids Res* **38**: D557–D562.

Freeman JD, Warren RL, Webb JR, Nelson BH, Holt RA. 2009. Profiling the T-cell receptor beta-chain repertoire by massively parallel sequencing. *Genome Res* **19**: 1817–1824.

Harty JT, Badovinac VP. 2008. Shaping and reshaping CD8 T cell memory. *Nat Rev Immunol* **8**: 107–119.

Johannesson A, Festin R. 1995. Phenotype transition of CD4+ T cells from CD45RA to CD45RO is accompanied by cell activation and proliferation. *Cytometry* **19**: 343–352.

Khor B, Sleckman BP. 2002. Allelic exclusion at the TCRbeta locus. *Curr Opin Immunol* **14**: 230–234.

Klarenbeek PL, Tak PP, van Schaik BD, Zwinderman AH, Jakobs ME, Zhang Z, van Kampen AH, van Lier RA, Baas F, de Vries N. 2010. Human T-cell memory consists mainly of unexpanded clones. *Immunol Lett* **133**: 42–48.

Larkin MA, Blackshields G, Brown NP, Chenna R, McGettigan PA, McWilliam H, Valentin F, Wallace IM, Wilm A, Lopez R, et al. 2007. Clustal W and Clustal X version 2.0. *Bioinformatics* **23**: 2947–2948.

Marsh SG, Albert ED, Bodmer WF, Bontrop RE, Dupont B, Erlich HA, Fernández-Viña M, Geraghty DE, Holdsworth R, Hurley CK, et al. 2010. Nomenclature for factors of the HLA system. 2010. *Tissue Antigens* **75**: 291–455.

Nikolic-Zugich J, Slifka MK, Messaoudi I. 2004. The many important facets of T-cell repertoire diversity. *Nat Rev Immunol* **4**: 123–132.

Ozawa T, Tajiri K, Kishi H, Muraguchi A. 2008. Comprehensive analysis of the functional TCR repertoire at the single-cell level. *Biochem Biophys Res Commun* **367**: 820–825.

Peters DG, Kassam AB, Yonas H, O'Hare EH, Ferrell RE, Brufsky AM. 1999. Comprehensive transcript analysis in small quantities of mRNA by SAGE-lite. *Nucleic Acids Res* **27**: e39. doi: 10.1093/nar/27.24.e39.

Robins HS, Campregher PV, Srivastava SK, Wacher A, Turtle CJ, Kahsai O, Riddell SR, Warren EH, Carlson CS. 2009. Comprehensive assessment of T-cell receptor β-chain diversity in αβ T cells. *Blood* **114**: 4099–4107.

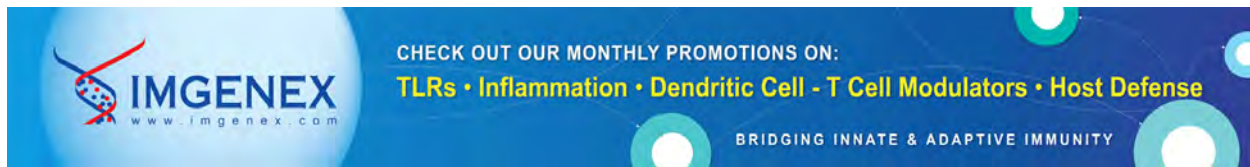
Robins HS, Srivastava SK, Campregher PV, Turtle CJ, Andriesen J, Riddell SR, Carlson CS, Warren EH. 2010. Overlap and effective size of the human CD8+ T cell receptor repertoire. *Sci Transl Med* **2**: 47ra64. doi: 10.1126/scitranslmed.3001442.

Robinson J, Waller MJ, Parham P, de Groot N, Bontrop R, Kennedy LJ, Stoehr P, Marsh SG. 2003. IMGT/HLA and IMGT/MHC: Sequence databases for the study of the major histocompatibility complex. *Nucleic Acids Res* **31**: 311–314.

Slater GS, Birney E. 2005. Automated generation of heuristics for biological sequence comparison. *BMC Bioinformatics* **6**: 31. doi: 10.1186/1471-2105-6-31.

Wang C, Sanders CM, Yang Q, Schroeder HW Jr, Wang E, Babrzadeh F, Gharizadeh, Myers B, Hudson RM Jr JR, Davis RW, et al. 2010. High throughput sequencing reveals a complex pattern of dynamic interrelationships among human T cell subsets. *Proc Natl Acad Sci* **107**: 1518–1523.

Received September 16, 2010; accepted in revised form December 28, 2010.



The Journal of Immunology

CD20+ B Cells: The Other Tumor-Infiltrating Lymphocytes

This information is current as of October 28, 2010

Brad H. Nelson

J. Immunol. 2010;185:4977-4982

doi:10.4049/jimmunol.1001323

<http://www.jimmunol.org/cgi/content/full/185/9/4977>

References

This article **cites 93 articles**, 40 of which can be accessed free at: <http://www.jimmunol.org/cgi/content/full/185/9/4977#BIBL>

Subscriptions

Information about subscribing to *The Journal of Immunology* is online at <http://www.jimmunol.org/subscriptions/>

Permissions

Submit copyright permission requests at <http://www.aai.org/ji/copyright.html>

Email Alerts

Receive free email alerts when new articles cite this article. Sign up at <http://www.jimmunol.org/subscriptions/etoc.shtml>

Downloaded from www.jimmunol.org on October 28, 2010

The Journal of Immunology is published twice each month by The American Association of Immunologists, Inc., 9650 Rockville Pike, Bethesda, MD 20814-3994. Copyright ©2010 by The American Association of Immunologists, Inc. All rights reserved. Print ISSN: 0022-1767 Online ISSN: 1550-6606.



CD20⁺ B Cells: The Other Tumor-Infiltrating Lymphocytes

Brad H. Nelson

Tumor-infiltrating CD8⁺ T cells are strongly associated with patient survival in a wide variety of human cancers. Less is known about tumor-infiltrating CD20⁺ B cells, which often colocalize with T cells, sometimes forming organized lymphoid structures. In autoimmunity and organ transplantation, T cells and B cells collaborate to generate potent, unrelenting immune responses that can result in extensive tissue damage and organ rejection. In these settings, B cells enhance T cell responses by producing Abs, stimulatory cytokines, and chemokines, serving as local APCs, and organizing the formation of tertiary lymphoid structures that sustain long-term immunity. Thus, B cells are an important component of immunological circuits associated with persistent, rampant tissue destruction. Engagement of tumor-reactive B cells may be an important condition for generating potent, long-term T cell responses against cancer. *The Journal of Immunology*, 2010, 185: 4977–4982.

The field of tumor immunology is strongly focused on CD8⁺ T cells, owing to their ability to directly kill tumor cells and the strong association between tumor-infiltrating CD8⁺ T cells and patient survival in many cancers (1). In contrast, B cells are often overlooked by tumor immunologists, likely because of the common notion that humoral and cytolytic responses work in opposition. Yet, B cells figure prominently in the fields of autoimmunity and tissue transplantation, settings in which T cell responses are so strong and persistent as to override the best attempts at immunosuppression. Given that the immune response to cancer develops over many years and, one hopes, can be manipulated to provide protection on a time scale of decades, there is undoubtedly much to be learned from the chronic immune responses seen in autoimmunity and transplantation. In this study, I will compare B cell responses in cancer, autoimmunity, and transplantation, with the goal of elucidating the mechanisms used by B cells to facilitate long-term T cell responses.

B cell development and differentiation

Human B cells develop in the bone marrow and initially have a naive phenotype manifested by unmutated Ig status, expression of IgM and IgD, and a CD27[−]CD38[−] surface phenotype (2). After activation by Ag, B cells enter primary follicles of lymph nodes or other lymphoid tissues where they undergo extensive proliferation, forming germinal centers (GCs) in which somatic hypermutation and class switching to IgG, IgA, or IgE take place. In the GCs, B cells receive growth and differentiation signals from follicular Th cells and compete for Ags presented by follicular dendritic cells (FDCs) in a process known as affinity maturation. B cells further differentiate into plasma cells (which produce high-affinity Abs) and long-lived CD27⁺CD38[−] memory cells (which respond to subsequent Ag encounters). CD20 is expressed on all mature B cells except plasma cells (3).

Although B cells typically reside in conventional lymphoid tissues such as spleen, lymph node, or blood, they can also be found in nonlymphoid tissues in aggregates with other immune cells. Such aggregates have been given various names but will be referred to here as tertiary lymphoid structures (TLSs). TLSs range from small aggregates of B cells, T cells, and DCs through to highly organized structures containing GCs, FDCs, T cell zones, high endothelial venules, and lymphatic vessels (4, 5). TLSs are found at sites of infection or inflammation in essentially any organ of the body and facilitate rapid and robust local immune responses (4, 5). As discussed later, TLSs are also seen in chronic immune responses associated with autoimmunity, allograft rejection, and cancer.

B cells in autoimmunity

In addition to their important role in immunity to pathogens, B cells contribute to various human autoimmune diseases through Ab-dependent and -independent mechanisms (6, 7). Autoantibodies contribute to autoimmune pathogenesis by inhibiting the function of their target proteins, activating the complement system, augmenting Ag presentation by DCs, or causing end-organ damage through the formation of immune complexes. In addition to making Abs, autoreactive B cells

Trev and Joyce Deeley Research Centre, British Columbia Cancer Agency; Department of Biochemistry and Microbiology, University of Victoria, Victoria; and Department of Medical Genetics, University of British Columbia, Vancouver, British Columbia, Canada

Received for publication June 23, 2010. Accepted for publication September 10, 2010.

This work was supported by the British Columbia Cancer Foundation.

Address correspondence and reprint requests to Dr. Brad H. Nelson, British Columbia Cancer Agency, 2410 Lee Avenue, Victoria, British Columbia V8R 6V5, Canada. E-mail address: bnelson@bccancer.bc.ca

Abbreviations used in this paper: AR, acute rejection; DC, dendritic cell; FDC, follicular dendritic cell; GC, germinal center; RA, rheumatoid arthritis; TIL, tumor-infiltrating lymphocyte; TIL-B, tumor-infiltrating B cell; TLS, tertiary lymphoid structure; Treg, regulatory T cell.

Copyright © 2010 by The American Association of Immunologists, Inc. 0022-1767/10/\$16.00

can enhance T cell responses through Ag presentation, co-stimulation, and modulation of DC migration and function (6, 7). For example, in the MRL/Mp-*lpr/lpr* model of lupus, mice that are genetically deficient in B cells not only fail to develop autoantibodies but also show greatly attenuated CD4⁺ and CD8⁺ T cell activation and reduced lymphocytic infiltration of end organs (8, 9).

Autoreactive B cells are found in TLSs in many autoimmune conditions, including rheumatoid arthritis (RA), Sjögren's syndrome, multiple sclerosis, autoimmune thyroiditis, diabetes, and lupus nephritis (4–6). In RA, TLSs are located in synovial tissue and serve as sites of clonal expansion, affinity maturation, and autoantibody production by B cells (7, 10–12). In a xenograft model in which affected synovial tissue from patients with RA was implanted in *scid* mice, depletion of synovial B cells lead to the disappearance of TLSs, reduced activation of T cells, and reduced levels of TNF- α and IFN- γ (13). Similarly, depletion of CD8⁺ T cells resulted in TLS disintegration and decreased lymphotxin and Ig secretion (14). Thus, B cells and T cells collaborate to maintain TLS structure and function.

The anti-CD20 mAb rituximab has been used to deplete B cells in various autoimmune conditions (6, 7). In RA, rituximab reduces autoantibodies as expected, yet it also benefits many autoantibody-negative patients by disrupting Ab-independent functions of B cells (7, 15). Specifically, rituximab causes the disappearance of TLSs, with concomitant loss of plasma cells, T cells, macrophages, and FDCs (16). Likewise, in patients with lupus, rituximab treatment results in decreased T cell activation and increased circulating regulatory T cells (Tregs) (15). In idiopathic thrombocytopenic purpura, rituximab can restore a normal CD4⁺ Th1/Th2 ratio (17). Finally, in multiple sclerosis, rituximab reduces the number of B and T cells in cerebral spinal fluid, with associated clinical benefit (18). Collectively, the use of rituximab in autoimmunity reveals a central role for B cells in the maintenance of pathological T cell responses.

B cells in allograft rejection

B cells also play a major role in allograft rejection. In a landmark study, renal allograft biopsies from patients undergoing acute rejection (AR) were subjected to gene expression profiling (19). As expected, there was a strong gene signature associated with T cells, NK cells, and macrophages. Unexpectedly, a B cell signature (including CD20, CD74, and Ig) was also prominent. By immunohistochemistry, ~40% of AR samples showed aggregates containing B cells, CD4⁺ T cells, CD8⁺ T cells, and macrophages (20). These aggregates were not associated with Ig or complement deposition, suggesting an Ab-independent role for B cells (19, 20). The presence of CD20⁺ B cells correlated with glucocorticoid resistance and graft loss. B cell infiltrates have also been described in human liver transplants undergoing AR (21), as well as cardiac transplants (22, 23).

B cells are thought to promote graft rejection by three major mechanisms (24). First, they produce donor-reactive Abs, which can damage tissue via complement and Ab-dependent cytotoxicity (23). Second, B cells produce cytokines and chemokines that can directly damage grafts as well as recruit T cells. Third, B cells can serve as APCs (25). For example,

in a mouse cardiac allograft model, B cells contributed to graft rejection by presenting alloantigens to CD4⁺ T cells (26).

Depletion of CD20⁺ B cells with rituximab can ameliorate renal allograft rejection (27–31). Not only does rituximab reduce CD20⁺ B cell aggregates in kidney tissue, it reduces expression of T cell-associated gene products such as OX40, Fas ligand, and granzyme B (29, 30). Thus, as in autoimmunity, B cells appear to facilitate pathological T cell responses against tissue allografts.

B cells in cancer

In contrast to the above findings in autoimmunity and transplantation, initial studies in mouse tumor models suggested that B cells generally inhibit T cell responses. For example, studies comparing wild-type and B cell-deficient mice found that B cells inhibit T cell-mediated regression of established tumors (32, 33), as well as T cell responses to cancer vaccines (34–36). B cells can impair the priming of CD8⁺ CTL responses by CD4⁺ T cells and instead promote non-protective humoral immune responses (37). Notably, however, other murine tumor studies have shown positive effects of B cells on T cell responses (38, 39). How can these conflicting results be reconciled? A key factor may be the activation status of B cells in different contexts, as T cell responses appear to be inhibited by resting B cells but facilitated by activated B cells (25, 40). Thus, studies in B cell-deficient mice, which lack both resting and activated B cells, could potentially yield conflicting results depending on the extent of B cell activation in the particular model system. As described below, B cells are commonly activated in human cancer patients, raising the possibility they play a positive role in tumor immunity.

Since the advent of serological cloning methods, it is now recognized that the majority of human cancer patients mount tumor-specific autoantibody responses (41). A wide variety of tumor Ags are recognized, including overexpressed proteins (e.g., HER-2/neu), aberrantly expressed proteins (e.g., cancer-testis Ags), and a plethora of apparently normal self-proteins (41, 42). Furthermore, standard treatments for cancer, such as hormone and radiation therapy, can trigger additional autoantibody responses, presumably through presentation of dying tumor cells to the immune system (43).

Tumor-infiltrating B cells (TIL-Bs) are another important aspect of the B cell response to cancer. TIL-Bs have been studied most extensively in breast cancer, where they are present in ~25% of tumors and comprise up to 40% of the tumor-infiltrating lymphocyte (TIL) population (42, 44, 45). TIL-Bs are often found in TLSs together with CD4⁺ and CD8⁺ T cells and DCs (46–48). TIL-Bs appear early during breast tumorigenesis, being present at the ductal carcinoma *in situ* stage (49). TIL-Bs generally express IgG and show evidence of Ag-driven expansion and somatic mutation consistent with affinity maturation (50–55). In one IgG sequencing study, >45% of TIL-B belonged to a clonal group, and there were 4–11 major clonal groups per tumor (46). In node-negative breast cancer, a gene signature indicative of TIL-B was positively associated with survival (56). Likewise, together with CD8⁺ and CD4⁺ T cells, TIL-Bs have been implicated in favorable survival rates in medullary breast cancer (42, 57, 58).

CD20⁺ TIL-Bs are also found in >40% of high-grade serous ovarian cancers, where they are associated with CD4⁺

and CD8⁺ T cells, as well as functional T cell markers such as TIA-1, granzyme B, and FoxP3 (59). TIL-Bs are strongly correlated with survival in ovarian cancer (59). Notably, tumors containing both CD8⁺ and CD20⁺ TILs are associated with higher survival than tumors containing CD8⁺ or CD20⁺ TILs alone, suggesting cooperative interactions between CD8⁺ and CD20⁺ TILs.

In non-small cell lung cancer, CD20⁺, CD8⁺, and CD4⁺ TILs are associated with increased survival (60, 61), as are TLS containing B cells, T cells, and mature DCs (62). TLS containing B cells, CD4⁺ and CD8⁺ T cells, and DCs are also found in colorectal cancer (63, 64). In cervical cancer, CD20⁺, CD4⁺, and CD8⁺ TILs are associated with a lower relapse rate (65). Finally, TIL-B are prominent in germ cell tumors, where they show evidence of Ag-driven clonal expansion and affinity maturation (66).

Considerable effort has gone into characterizing the target Ags of TIL-B. In a large study of various human cancers, TIL-B-derived autoantibodies were shown to react primarily with autologous tumor targets or allogeneic tumors of the same tissue type, suggesting they recognized tumor-associated Ags (67). In medullary breast cancer, TIL-B-derived autoantibodies were shown to recognize ganglioside D3 and β -actin, the latter by virtue of exposure of β -actin on the surface of apoptotic tumor cells (54, 55, 68). In lung cancer, target Ags of TIL-B include p53, as well as many self-Ags that are overexpressed in tumor tissue (69).

In summary, TIL-Bs are prevalent in human cancer, recognize a wide variety of tumor and self-Ags, associate closely with T cells and other immune cells, and correlate with favorable outcomes. This provides clear rationale to better understand their mechanistic properties.

Mechanisms of action of TIL-B

Although little is known about the mechanisms by which TIL-B promote favorable outcomes in cancer, several possibilities are suggested by studies in autoimmunity, transplantation, and various experimental models (Fig. 1).

TIL-B-derived autoantibodies

As mentioned, autoantibodies and alloreactive Abs play major pathogenic roles in autoimmunity and transplantation, respectively. Similarly, TIL-Bs could potentially mediate their effects through autoantibodies, which could directly modulate the function of target proteins, or promote tumor immunity through the opsonization of tumor Ags, complement-mediated destruction of tumor cells, or Ab-dependent cytotoxicity. For

example, in a murine study, adoptively transferred B cells promoted tumor rejection by producing complement-fixing, tumor-reactive Abs (70). Furthermore, the induction of autoantibody responses in mice through vaccination was shown to enhance CD8⁺ T cell responses against tumors (71). However, in human cancer, the relationship between autoantibodies and clinical outcomes remains controversial. For instance, anti-p53 serum autoantibodies, arguably the best-studied example, have been linked to favorable outcomes in some studies, but not others (72). This inconsistency may be attributable to the generally low concentrations of tumor-reactive autoantibodies in serum (42). Perhaps TIL-Bs, by virtue of location, raise the local concentration of autoantibodies to physiologically significant levels at the tumor site. Consistent with this idea, when human lung cancer specimens were engrafted in *scid* mice, TIL-B-derived autoantibodies were associated with decreased tumor growth (73, 74).

Direct cytotoxicity by B cells

TIL-Bs might also directly kill tumor cells through Ab-independent mechanisms (75). When stimulated with IL-21, human B cells can secrete granzyme B (76), which could potentially have direct cytotoxicity against tumor cells. Moreover, human B cells stimulated with IFN- α or TLR agonist were shown to kill tumor cells directly via TRAIL signaling (77). Notably, however, cytokines derived from TIL-B can sometimes provide survival signals to tumor cells, as shown for lymphotoxin in murine prostate cancer (78).

Immunoregulation by B cells

Tumors typically contain complex mixtures of immune cells, which, in addition to TIL-Bs, can include cytotoxic T cells, Th cells (e.g., Th1, Th2, Th17), Tregs, DCs, and myeloid-derived suppressor cells. Thus, TIL-Bs could mediate their effects in part by regulating other immune cells. For example, under the influence of CD4⁺ Th1 and Th2 cells, B cells can be polarized into subsets that produce IFN- γ , IL-12, and TNF- α (Be-1 cells) or IL-2, IL-4, TNF- α , and IL-6 (Be-2 cells) (79, 80). Conversely, Be-1 and Be-2 cells can promote the differentiation of Th1 and Th2 cells, respectively, such that polarized cytokine profiles of both B cells and Th cells are amplified and maintained (79, 80). B cells also facilitate the formation of CD4⁺ T cell memory (81) and promote the survival and proliferation of activated CD8⁺ T cells through CD27-CD70 interactions (82). B cells also engage in negative regulatory relationships. For example, regulatory

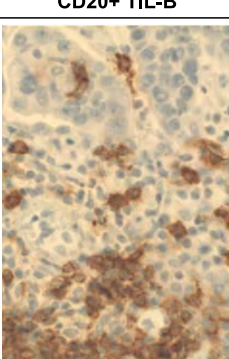
CD20 ⁺ TIL-B	Effect molecules	Potential mechanisms
	tumor-reactive autoantibodies	<ul style="list-style-type: none"> target protein inhibition opsonization complement ADCC
	cytokines, chemokines	<ul style="list-style-type: none"> Th1/Th2 polarization CD8⁺ T-cell proliferation DC migration and function TLS formation
	granzyme, TRAIL	<ul style="list-style-type: none"> direct tumor cell killing
	MHC class I and II, co-stimulatory molecules	<ul style="list-style-type: none"> antigen presentation to CD4⁺ and CD8⁺ T cells

FIGURE 1. Potential mechanisms by which TIL-B promote tumor immunity. *Left panel*, TIL-B in human ovarian cancer visualized by anti-CD20 immunohistochemistry (brown). Original magnification $\times 40$. *Center panel*, Effector molecules produced by B cells. *Right panel*, Potential TIL-B mechanisms involving either direct effects on tumor cells or enhancement of the antitumor activity of T cells and other immune cells.

B cells can dampen immune responses through secretion of IL-10 and TGF β -1 (7). Conversely, Tregs can inhibit B cell activation, proliferation, and Ab production (83).

In a striking example of immunoregulation, B cells can promote the formation of TLSs by secreting lymphotoxin and chemokines, which attract and stimulate T cells, DCs, and other immune cells (7, 82, 84, 85). Accordingly, elimination of B cells in RA or renal allografts results in the disintegration of TLSs with consequent diminution of T cell activity (13, 16, 29, 30). Because TLSs are associated with favorable outcomes in human cancer (62) and murine models (86), this likely represents a key immunoregulatory property of TIL-Bs.

Ag presentation by B cells

Activated B cells can serve as APCs for both CD4 $^+$ and CD8 $^+$ T cells (7, 25). Indeed, B cells have an advantage over DCs, as they can selectively present cognate Ag collected through surface Ig molecules, which allows presentation of even low concentrations of Ag. Moreover, B cells can indirectly enhance Ag presentation by other APCs through production of specific Ab (87). The relative contributions of DCs and B cells to Ag presentation *in vivo* depends on context. In general, it appears DCs are important for initial T cell priming, whereas B cells may promote T cell expansion and memory formation (7, 25, 88).

Why might B cells be required as APCs at the tumor site? T cell activation and expansion are initiated by DCs in draining lymph nodes, yet there is growing recognition from viral models that optimal responses require a second wave of T cell proliferation triggered by APCs at the site of infection (89, 90). This process may be particularly important during prolonged or chronic immune responses (89). Whereas DCs might serve as effective APCs initially, one can imagine that with time, DCs may decline in number or become diverted to a suppressive phenotype, especially in the tumor environment. Although speculative, perhaps TIL-Bs can serve as local APCs under these circumstances, thereby sustaining the survival and proliferation of tumor-infiltrating T cells over the long term. Consistent with this, we found that advanced ovarian cancers lack intratumoral DCs and instead contain TIL-Bs in close association with T cells (59).

Conclusions

The autoimmunity and transplantation fields have exposed B cells as key players in chronic, recalcitrant T cell responses. In addition to direct effects against tissues through Abs or cytotoxic pathways, B cells can promote T cell responses by producing cytokines and chemokines, facilitating TLS formation, and serving as APCs (Fig. 1). The contribution of B cells to tumor immunity might not be evident in many murine tumor models, which tend to involve rapid cytolytic responses akin to acute viral infections. By contrast, in human cancer, the beneficial effects of TILs on clinical outcomes extend over many years, which is more consistent with a chronic immune process. From this perspective, how can we best engage B cells for cancer therapy? The Ab-mediated effects of TIL-Bs can potentially be mimicked by therapeutic mAbs, which represent a rapidly expanding class of cancer drugs. Furthermore, cell-based cancer vaccines can be used to elicit broader Ab responses that closely resemble those associated with naturally occurring TIL-Bs. For example, in

melanoma and prostate cancer patients receiving cell-based vaccines expressing GM-CSF, the development of autoantibodies to self-antigens was associated with favorable clinical responses (91–93). It is less clear how best to enhance the immunoregulatory and Ag presentation functions of TIL-Bs. Models are needed in which TIL-Bs and T cells collaborate to provide long-term tumor control, as opposed to the models of acute rejection used by most investigators. To this end, TIL populations have been shown to persist for weeks to months in the most current tumor xenograft models (94), providing an experimental system to study functional interactions between TIL-Bs and other cell types. Additional insights will undoubtedly continue to emerge from the autoimmunity and transplantation fields through their continued efforts to disrupt the complex and powerful interactions between B cells and T cells.

Acknowledgments

I thank the patients, clinicians, and researchers who contributed to the studies reviewed in this paper, Katy Milne for help with Fig. 1, and members of the Deeley Research Centre for helpful discussions.

Disclosures

The author has no financial conflicts of interest.

References

1. Pagès, F., J. Galon, M. C. Dieu-Nosjean, E. Tartour, C. Sautès-Fridman, and W. H. Fridman. 2010. Immune infiltration in human tumors: a prognostic factor that should not be ignored. *Oncogene* 29: 1093–1102.
2. Schmidlin, H., S. A. Diehl, and B. Blom. 2009. New insights into the regulation of human B-cell differentiation. *Trends Immunol.* 30: 277–285.
3. DiLillo, D. J., Y. Hamaguchi, Y. Ueda, K. Yang, J. Uchida, K. M. Haas, G. Kelsoe, and T. F. Tedder. 2008. Maintenance of long-lived plasma cells and serological memory despite mature and memory B cell depletion during CD20 immunotherapy in mice. *J. Immunol.* 180: 361–371.
4. Drayton, D. L., S. Liao, R. H. Mounzer, and N. H. Ruddle. 2006. Lymphoid organ development: from ontogeny to neogenesis. *Nat. Immunol.* 7: 344–353.
5. Carragher, D. M., J. Rangel-Moreno, and T. D. Randall. 2008. Ectopic lymphoid tissues and local immunity. *Semin. Immunol.* 20: 26–42.
6. Martin, F., and A. C. Chan. 2006. B cell immunobiology in disease: evolving concepts from the clinic. *Annu. Rev. Immunol.* 24: 467–496.
7. Yanaba, K., J. D. Bouaziz, T. Matsushita, C. M. Magro, E. W. St Clair, and T. F. Tedder. 2008. B-lymphocyte contributions to human autoimmune disease. *Immunol. Rev.* 223: 284–299.
8. Chan, O., and M. J. Shlomchik. 1998. A new role for B cells in systemic autoimmunity: B cells promote spontaneous T cell activation in MRL-lpr/lpr mice. *J. Immunol.* 160: 51–59.
9. Chan, O. T., M. P. Madaio, and M. J. Shlomchik. 1999. B cells are required for lupus nephritis in the polygenic, Fas-intact MRL model of systemic autoimmunity. *J. Immunol.* 163: 3592–3596.
10. Gause, A., K. Gundlach, M. Zdichavsky, G. Jacobs, B. Koch, T. Hopf, and M. Pfreundschuh. 1995. The B lymphocyte in rheumatoid arthritis: analysis of rearranged V kappa genes from B cells infiltrating the synovial membrane. *Eur. J. Immunol.* 25: 2775–2782.
11. Itoh, K., V. Patki, R. A. Furie, E. K. Chartash, R. I. Jain, L. Lane, S. E. Asnis, and N. Chiorazzi. 2000. Clonal expansion is a characteristic feature of the B-cell repertoire of patients with rheumatoid arthritis. *Arthritis Res.* 2: 50–58.
12. Humby, F., M. Bombardieri, A. Manzo, S. Kelly, M. C. Blades, B. Kirkham, J. Spencer, and C. Pitzalis. 2009. Ectopic lymphoid structures support ongoing production of class-switched autoantibodies in rheumatoid synovium. *PLoS Med.* 6: e1.
13. Takemura, S., P. A. Klimiuk, A. Braun, J. J. Goronzy, and C. M. Weyand. 2001. T cell activation in rheumatoid synovium is B cell dependent. *J. Immunol.* 167: 4710–4718.
14. Kang, Y. M., X. Zhang, U. G. Wagner, H. Yang, R. D. Beckenbaugh, P. J. Kurtin, J. J. Goronzy, and C. M. Weyand. 2002. CD8 T cells are required for the formation of ectopic germinal centers in rheumatoid synovitis. *J. Exp. Med.* 195: 1325–1336.
15. Liassis, S. N., and P. P. Sfikakis. 2008. Rituximab-induced B cell depletion in autoimmune diseases: potential effects on T cells. *Clin. Immunol.* 127: 280–285.
16. Thurlings, R. M., K. Vos, C. A. Wijbrandts, A. H. Zwinderman, D. M. Gerlag, and P. P. Tak. 2008. Synovial tissue response to rituximab: mechanism of action and identification of biomarkers of response. *Ann. Rheum. Dis.* 67: 917–925.
17. Stasi, R., G. Del Poeta, E. Stipa, M. L. Evangelista, M. M. Trawinska, N. Cooper, and S. Amadori. 2007. Response to B-cell depleting therapy with rituximab reverts the abnormalities of T-cell subsets in patients with idiopathic thrombocytopenic purpura. *Blood* 110: 2924–2930.

18. Cross, A. H., J. L. Stark, J. Lauber, M. J. Ramsbottom, and J. A. Lyons. 2006. Rituximab reduces B cells and T cells in cerebrospinal fluid of multiple sclerosis patients. *J. Neuroimmunol.* 180: 63–70.

19. Sarwal, M., M. S. Chua, N. Kambham, S. C. Hsieh, T. Satterwhite, M. Masek, and O. Salvatierra Jr. 2003. Molecular heterogeneity in acute renal allograft rejection identified by DNA microarray profiling. *N. Engl. J. Med.* 349: 125–138.

20. Zarkhin, V., N. Kambham, L. Li, S. Kwok, S. C. Hsieh, O. Salvatierra, and M. M. Sarwal. 2008. Characterization of intra-graft B cells during renal allograft rejection. *Kidney Int.* 74: 664–673.

21. Kruckemeyer, M. G., J. Moeller, L. Morawietz, B. Rudolph, U. Neumann, T. Theruvath, P. Neuhaus, and V. Krenn. 2004. Description of B lymphocytes and plasma cells, complement, and chemokines/receptors in acute liver allograft rejection. *Transplantation* 78: 65–70.

22. Michaels, P. J., J. Kobashigawa, H. Laks, A. Azarbal, M. L. Espejo, L. Chen, and M. C. Fishbein. 2001. Differential expression of RANTES chemokine, TGF- β , and leukocyte phenotype in acute cellular rejection and quilty B lesions. *J. Heart Lung Transplant.* 20: 407–416.

23. Thaunat, O., A. C. Field, J. Dai, L. Louedec, N. Patey, M. F. Bloch, C. Mandet, M. F. Belair, P. Brunet, O. Meilhac, et al. 2005. Lymphoid neogenesis in chronic rejection: evidence for a local humoral alloimmune response. *Proc. Natl. Acad. Sci. USA* 102: 14723–14728.

24. Zarkhin, V., L. Li, and M. Sarwal. 2008. "To B or not to B?" B-cells and graft rejection. *Transplantation* 85: 1705–1714.

25. Rodríguez-Pinto, D. 2005. B cells as antigen presenting cells. *Cell. Immunol.* 238: 67–75.

26. Noorchashm, H., A. J. Reed, S. Y. Rostami, R. Mozaffari, G. Zekavat, B. Koerberlein, A. J. Caton, and A. Naji. 2006. B cell-mediated antigen presentation is required for the pathogenesis of acute cardiac allograft rejection. *J. Immunol.* 177: 7715–7722.

27. Becker, Y. T., B. N. Becker, J. D. Pirsch, and H. W. Sollinger. 2004. Rituximab as treatment for refractory kidney transplant rejection. *Am. J. Transplant.* 4: 996–1001.

28. Alausa, M., U. Almagro, N. Siddiqui, R. Zuiderweg, R. Medipalli, and S. Hariharan. 2005. Refractory acute kidney transplant rejection with CD20 graft infiltrates and successful therapy with rituximab. *Clin. Transplant.* 19: 137–140.

29. Gengenbarg, H., A. Hansson, A. Wernerson, L. Wennberg, and G. Tydén. 2006. Pharmacodynamics of rituximab in kidney allograft transplantation. *Am. J. Transplant.* 6: 2418–2428.

30. Lehnhardt, A., M. Mengel, L. Pape, J. H. Ehrlich, G. Offner, and J. Strehlau. 2006. Nodular B-cell aggregates associated with treatment refractory renal transplant rejection resolved by rituximab. *Am. J. Transplant.* 6: 847–851.

31. Zarkhin, V., L. Li, N. Kambham, T. Sigdel, O. Salvatierra, and M. M. Sarwal. 2008. A randomized, prospective trial of rituximab for acute rejection in pediatric renal transplantation. *Am. J. Transplant.* 8: 2607–2617.

32. Shah, S., A. A. Divekar, S. P. Hilchey, H. M. Cho, C. L. Newman, S. U. Shin, H. Nechustan, P. M. Challita-Eid, B. M. Segal, K. H. Yi, and J. D. Rosenblatt. 2005. Increased rejection of primary tumors in mice lacking B cells: inhibition of anti-tumor CTL and TH1 cytokine responses by B cells. *Int. J. Cancer* 117: 574–586.

33. Barbera-Guillem, E., M. B. Nelson, B. Barr, J. K. Nyhus, K. F. May Jr., L. Feng, and J. W. Sampsel. 2000. B lymphocyte pathology in human colorectal cancer. Experimental and clinical therapeutic effects of partial B cell depletion. *Cancer Immunol. Immunother.* 48: 541–549.

34. Oizumi, S., V. Deyev, K. Yamazaki, T. Schreiber, N. Strbo, J. Rosenblatt, and E. R. Podack. 2008. Surmounting tumor-induced immune suppression by frequent vaccination or immunization in the absence of B cells. *J. Immunother.* 31: 394–401.

35. Perricone, M. A., K. A. Smith, K. A. Claussen, M. S. Plog, D. M. Hempel, B. L. Roberts, J. A. St George, and J. M. Kaplan. 2004. Enhanced efficacy of melanoma vaccines in the absence of B lymphocytes. *J. Immunother.* 27: 273–281.

36. Kim, S., Z. G. Fridlender, R. Dunn, M. R. Kehry, V. Kapoor, A. Blouin, L. R. Kaiser, and S. M. Albelda. 2008. B-cell depletion using an anti-CD20 antibody augments antitumor immune responses and immunotherapy in nonhematopoietic murine tumor models. *J. Immunother.* 31: 446–457.

37. Qin, Z., G. Richter, T. Schüller, S. Ibe, X. Cao, and T. Blankenstein. 1998. B cells inhibit induction of T cell-dependent tumor immunity. *Nat. Med.* 4: 627–630.

38. Schultz, K. R., J. P. Klarnet, R. S. Gieni, K. T. HayGlass, and P. D. Greenberg. 1990. The role of B cells for in vivo T cell responses to a Friend virus-induced leukemia. *Science* 249: 921–923.

39. DiLillo, D. J., K. Yanaba, and T. F. Tedder. 2010. B cells are required for optimal CD4+ and CD8+ T cell tumor immunity: therapeutic B cell depletion enhances B16 melanoma growth in mice. *J. Immunol.* 184: 4006–4016.

40. Watt, V., F. Ronchese, and D. Ritchie. 2007. Resting B cells suppress tumor immunity via an MHC class-II dependent mechanism. *J. Immunother.* 30: 323–332.

41. Reuschenbach, M., M. von Knebel Doeberitz, and N. Wentzzen. 2009. A systematic review of humoral immune responses against tumor antigens. *Cancer Immunol. Immunother.* 58: 1535–1544.

42. Coronella-Wood, J. A., and E. M. Hersh. 2003. Naturally occurring B-cell responses to breast cancer. *Cancer Immunol. Immunother.* 52: 715–738.

43. Nesslinger, N. J., R. A. Sahota, B. Stone, K. Johnson, N. Chima, C. King, D. Rasmussen, D. Bishop, P. S. Rennie, M. Gleave, et al. 2007. Standard treatments induce antigen-specific immune responses in prostate cancer. *Clin. Cancer Res.* 13: 1493–1502.

44. Chin, Y., J. Janseens, J. Vandepitte, J. Vandendbran, L. Opdebeek, and J. Raus. 1992. Phenotypic analysis of tumor-infiltrating lymphocytes from human breast cancer. *Anticancer Res.* 12: 1463–1466.

45. Marsigliante, S., L. Biscozzo, A. Marra, G. Nicolardi, G. Leo, G. B. Lobreglio, and C. Storelli. 1999. Computerised counting of tumour infiltrating lymphocytes in 90 breast cancer specimens. *Cancer Lett.* 139: 33–41.

46. Coronella, J. A., C. Spier, M. Welch, K. T. Trevor, A. T. Stopeck, H. Villar, and E. M. Hersh. 2002. Antigen-driven oligoclonal expansion of tumor-infiltrating B cells in infiltrating ductal carcinoma of the breast. *J. Immunol.* 169: 1829–1836.

47. Yakirevich, E., O. B. Izhak, G. Rennert, Z. G. Kovacs, and M. B. Resnick. 1999. Cytotoxic phenotype of tumor infiltrating lymphocytes in medullary carcinoma of the breast. *Mod. Pathol.* 12: 1050–1056.

48. Tamiolakis, D., C. Simopoulos, A. Cheva, M. Lambropoulou, A. Kotini, T. Jivannakis, and N. Papadopoulos. 2002. Immunophenotypic profile of tumor infiltrating lymphocytes in medullary carcinoma of the breast. *Eur. J. Gynaecol. Oncol.* 23: 433–436.

49. Lee, A. H., L. C. Happerfield, L. G. Bobrow, and R. R. Millis. 1997. Angiogenesis and inflammation in ductal carcinoma in situ of the breast. *J. Pathol.* 181: 200–206.

50. Wang, Y., F. Ylera, M. Boston, S. G. Kang, J. L. Kuto, A. J. Klein-Szanto, and R. P. Junghans. 2007. Focused antibody response in plasma cell-infiltrated non-medullary (NOS) breast cancers. *Breast Cancer Res. Treat.* 104: 129–144.

51. Simas, P., J. L. Teillaud, D. I. Stott, J. Tóth, and B. Kotlan. 2005. Tumor-infiltrating B cell immunoglobulin variable region gene usage in invasive ductal breast carcinoma. *Pathol. Oncol. Res.* 11: 92–97.

52. Nzula, S., J. Goings, and D. I. Stott. 2003. Antigen-driven clonal proliferation, somatic hypermutation, and selection of B lymphocytes infiltrating human ductal breast carcinomas. *Cancer Res.* 63: 3275–3280.

53. Coronella, J. A., P. Telleman, G. A. Kingsbury, T. D. Truong, S. Hays, and R. P. Junghans. 2001. Evidence for an antigen-driven humoral immune response in medullary ductal breast cancer. *Cancer Res.* 61: 7889–7899.

54. Hansen, M. H., H. V. Nielsen, and H. J. Ditzel. 2002. Translocation of an intracellular antigen to the surface of medullary breast cancer cells early in apoptosis allows for an antigen-driven antibody response elicited by tumor-infiltrating B cells. *J. Immunol.* 169: 2701–2711.

55. Hansen, M. H., H. Nielsen, and H. J. Ditzel. 2001. The tumor-infiltrating B cell response in medullary breast cancer is oligoclonal and directed against the autoantigen actin exposed on the surface of apoptotic cancer cells. *Proc. Natl. Acad. Sci. USA* 98: 12659–12664.

56. Schmidt, M., D. Böhm, C. von Törne, E. Steiner, A. Puhl, H. Pilch, H. A. Lehr, J. G. Hengstler, H. Kölbl, and M. Gehrmann. 2008. The humoral immune system has a key prognostic impact in node-negative breast cancer. *Cancer Res.* 68: 5405–5413.

57. Ridolfi, R. L., P. P. Rosen, A. Port, D. Kinne, and V. Miké. 1977. Medullary carcinoma of the breast: a clinicopathologic study with 10 year follow-up. *Cancer* 40: 1365–1385.

58. Lim, K. H., P. U. Telisinghe, M. S. Abdullah, and R. Ramasamy. 2010. Possible significance of differences in proportions of cytotoxic T cells and B-lineage cells in the tumour-infiltrating lymphocytes of typical and atypical medullary carcinomas of the breast. *Cancer Immun.* 10: 3.

59. Milne, K., M. Köbel, S. E. Kalloger, R. O. Barnes, D. Gao, C. B. Gilks, P. H. Watson, and B. H. Nelson. 2009. Systematic analysis of immune infiltrates in high-grade serous ovarian cancer reveals CD20, FoxP3 and TIA-1 as positive prognostic factors. *PLoS ONE* 4: e6412.

60. Al-Shibli, K. I., T. Donnem, S. Al-Saad, M. Persson, R. M. Bremnes, and L. T. Busund. 2008. Prognostic effect of epithelial and stromal lymphocyte infiltration in non-small cell lung cancer. *Clin. Cancer Res.* 14: 5220–5227.

61. Riemann, D., K. Wenzel, T. Schulz, S. Hofmann, H. Neef, C. Lautenschläger, and J. Langner. 1997. Phenotypic analysis of T lymphocytes isolated from non-small-cell lung cancer. *Int. Arch. Allergy Immunol.* 114: 38–45.

62. Dieu-Nosjean, M. C., M. Antoine, C. Daniel, D. Heudes, M. Wislez, V. Poulot, N. Rabie, L. Laurans, E. Tartour, L. de Chaisemartin, et al. 2008. Long-term survival for patients with non-small-cell lung cancer with intratumoral lymphoid structures. *J. Clin. Oncol.* 26: 4410–4417.

63. Suzuki, A., A. Masuda, H. Nagata, S. Kameoka, Y. Kikawada, M. Yamakawa, and T. Kasajima. 2002. Mature dendritic cells make clusters with T cells in the invasive margin of colorectal carcinoma. *J. Pathol.* 196: 37–43.

64. Jackson, P. A., M. A. Green, C. G. Marks, R. J. King, R. Hubbard, and M. G. Cook. 1996. Lymphocyte subset infiltration patterns and HLA antigen status in colorectal carcinomas and adenomas. *Gut* 38: 85–89.

65. Nedergaard, B. S., M. Ladekarl, J. R. Nyengaard, and K. Nielsen. 2008. A comparative study of the cellular immune response in patients with stage IB cervical squamous cell carcinoma. Low numbers of several immune cell subtypes are strongly associated with relapse of disease within 5 years. *Gynecol. Oncol.* 108: 106–111.

66. Willis, S. N., S. S. Mallozzi, S. J. Rodig, K. M. Cronk, S. L. McArdle, T. Caron, G. S. Pinkus, L. Lovato, K. L. Shampain, D. E. Anderson, et al. 2009. The microenvironment of germ cell tumors harbors a prominent antigen-driven humoral response. *J. Immunol.* 182: 3310–3317.

67. Punt, C. J., J. A. Barbuto, H. Zhang, W. J. Grimes, K. D. Hatch, and E. M. Hersh. 1994. Anti-tumor antibody produced by human tumor-infiltrating and peripheral blood B lymphocytes. *Cancer Immunol. Immunother.* 38: 225–232.

68. Kotlan, B., P. Simas, J. L. Teillaud, W. H. Fridman, J. Toth, M. McKnight, and M. C. Glassy. 2005. Novel ganglioside antigen identified by B cells in human medullary breast carcinomas: the proof of principle concerning the tumor-infiltrating B lymphocytes. *J. Immunol.* 175: 2278–2285.

69. Yasuda, M., M. Mizukami, T. Hanagiri, Y. Shigematsu, T. Fukuyama, Y. Nagata, T. So, Y. Ichiki, M. Sugaya, M. Takenoyama, et al. 2006. Antigens recognized by IgG derived from tumor-infiltrating B lymphocytes in human lung cancer. *Anticancer Res.* 26(5A): 3607–3611.

70. Li, Q., S. Teitz-Tennenbaum, E. J. Donald, M. Li, and A. E. Chang. 2009. In vivo sensitized and in vitro activated B cells mediate tumor regression in cancer adoptive immunotherapy. *J. Immunol.* 183: 3195–3203.

71. Nishikawa, H., K. Tanida, H. Ikeda, M. Sakakura, Y. Miyahara, T. Aota, K. Mukai, M. Watanabe, K. Kuribayashi, L. J. Old, and H. Shiku. 2001. Role of SEREX-

defined immunogenic wild-type cellular molecules in the development of tumor-specific immunity. *Proc. Natl. Acad. Sci. USA* 98: 14571–14576.

72. Kumar, S., A. Mohan, and R. Guleria. 2009. Prognostic implications of circulating anti-p53 antibodies in lung cancer—a review. *Eur. J. Cancer Care (Engl.)* 18: 248–254.

73. Mizukami, M., T. Hanagiri, Y. Shigematsu, T. Baba, T. Fukuyama, Y. Nagata, T. So, Y. Ichiki, M. Sugaya, M. Yasuda, et al. 2006. Effect of IgG produced by tumor-infiltrating B lymphocytes on lung tumor growth. *Anticancer Res.* 26(3A): 1827–1831.

74. Williams, S. S., F. A. Chen, H. Kida, S. Yokata, K. Miya, M. Kato, M. P. Barcos, H. Q. Wang, T. Alosco, T. Umemoto, et al. 1996. Engraftment of human tumor-infiltrating lymphocytes and the production of anti-tumor antibodies in SCID mice. *J. Immunol.* 156: 1908–1915.

75. Lundy, S. K. 2009. Killer B lymphocytes: the evidence and the potential. *Inflamm. Res.* In press.

76. Hagn, M., E. Schwesinger, V. Ebel, K. Sontheimer, J. Maier, T. Beyer, T. Syrovets, Y. Laumonnier, D. Fabricius, T. Simmet, and B. Jahrsdörfer. 2009. Human B cells secrete granzyme B when recognizing viral antigens in the context of the acute phase cytokine IL-21. *J. Immunol.* 183: 1838–1845.

77. Kemp, T. J., J. M. Moore, and T. S. Griffith. 2004. Human B cells express functional TRAIL/Apo-2 ligand after CpG-containing oligodeoxynucleotide stimulation. *J. Immunol.* 173: 892–899.

78. Ammirante, M., J. L. Luo, S. Grivennikov, S. Nedospasov, and M. Karin. 2010. B-cell-derived lymphotoxin promotes castration-resistant prostate cancer. *Nature* 464: 302–305.

79. Harris, D. P., L. Haynes, P. C. Sayles, D. K. Duso, S. M. Eaton, N. M. Lepak, L. L. Johnson, S. L. Swain, and F. E. Lund. 2000. Reciprocal regulation of polarized cytokine production by effector B and T cells. *Nat. Immunol.* 1: 475–482.

80. Lund, F. E. 2008. Cytokine-producing B lymphocytes—key regulators of immunity. *Curr. Opin. Immunol.* 20: 332–338.

81. Whitmire, J. K., M. S. Asano, S. M. Kaech, S. Sarkar, L. G. Hannum, M. J. Shlomchik, and R. Ahmed. 2009. Requirement of B cells for generating CD4+ T cell memory. *J. Immunol.* 182: 1868–1876.

82. Deola, S., M. C. Panelli, D. Maric, S. Selleri, N. I. Dmitrieva, C. Y. Voss, H. Klein, D. Stroncek, E. Wang, and F. M. Marincola. 2008. Helper B cells promote cytotoxic T cell survival and proliferation independently of antigen presentation through CD27/CD70 interactions. *J. Immunol.* 180: 1362–1372.

83. Kim, C. H. 2006. Regulation of humoral immunity by FoxP3+ regulatory T cells. *Expert Rev. Clin. Immunol.* 2: 859–868.

84. Schaniel, C., E. Pardali, F. Sallusto, M. Spelejas, C. Ruedl, T. Shimizu, T. Seidl, J. Andersson, F. Melchers, A. G. Rolink, and P. Sideras. 1998. Activated murine B lymphocytes and dendritic cells produce a novel CC chemokine which acts selectively on activated T cells. *J. Exp. Med.* 188: 451–463.

85. Bystry, R. S., V. Aluvihare, K. A. Welch, M. Kallikourdis, and A. G. Betz. 2001. B cells and professional APCs recruit regulatory T cells via CCL4. *Nat. Immunol.* 2: 1126–1132.

86. Schrama, D., P. Thor Straten, W. H. Fischer, A. D. McLellan, E. B. Bröcker, R. A. Reisfeld, and J. C. Becker. 2001. Targeting of lymphotoxin-alpha to the tumor elicits an efficient immune response associated with induction of peripheral lymphoid-like tissue. *Immunity* 14: 111–121.

87. Kurt-Jones, E. A., D. Liano, K. A. HayGlass, B. Benacerraf, M. S. Sy, and A. K. Abbas. 1988. The role of antigen-presenting B cells in T cell priming in vivo. Studies of B cell-deficient mice. *J. Immunol.* 140: 3773–3778.

88. Bouaziz, J. D., K. Yanaba, G. M. Venturi, Y. Wang, R. M. Tisch, J. C. Poe, and T. F. Tedder. 2007. Therapeutic B cell depletion impairs adaptive and autoreactive CD4+ T cell activation in mice. *Proc. Natl. Acad. Sci. USA* 104: 20878–20883.

89. Wakim, L. M., J. Waithman, N. van Rooijen, W. R. Heath, and F. R. Carbone. 2008. Dendritic cell-induced memory T cell activation in nonlymphoid tissues. *Science* 319: 198–202.

90. McGill, J., N. Van Rooijen, and K. L. Legge. 2008. Protective influenza-specific CD8 T cell responses require interactions with dendritic cells in the lungs. *J. Exp. Med.* 205: 1635–1646.

91. Urba, W. J., J. Nemunaitis, F. Marshall, D. C. Smith, K. M. Hege, J. Ma, M. Nguyen, and E. J. Small. 2008. Treatment of biochemical recurrence of prostate cancer with granulocyte-macrophage colony-stimulating factor secreting, allogeneic, cellular immunotherapy. *J. Urol.* 180: 2011–2017; discussion 2017–2018.

92. Hodi, F. S., J. C. Schmollinger, R. J. Soiffer, R. Salgia, T. Lynch, J. Ritz, E. P. Alyea, J. Yang, D. Neuberg, M. Mihm, and G. Dranoff. 2002. ATP6S1 elicits potent humoral responses associated with immune-mediated tumor destruction. *Proc. Natl. Acad. Sci. USA* 99: 6919–6924.

93. Sittler, T., J. Zhou, J. Park, N. K. Yuen, S. Sarantopoulos, J. Mollick, R. Salgia, A. Giobbe-Hurder, G. Dranoff, and F. S. Hodi. 2008. Concerted potent humoral immune responses to autoantigens are associated with tumor destruction and favorable clinical outcomes without autoimmunity. *Clin. Cancer Res.* 14: 3896–3905.

94. Simpson-Abelson, M. R., G. F. Sonnenberg, H. Takita, S. J. Yokota, T. F. Conway Jr., R. J. Kelleher Jr., L. D. Shultz, M. Barcos, and R. B. Bankert. 2008. Long-term engraftment and expansion of tumor-derived memory T cells following the implantation of non-disrupted pieces of human lung tumor into NOD-scid IL2R γ (null) mice. *J. Immunol.* 180: 7009–7018.



Contents lists available at ScienceDirect

Journal of Immunological Methods

journal homepage: www.elsevier.com/locate/jim

Research paper

An *in vitro*-transcribed-mRNA polyepitope construct encoding 32 distinct HLA class I-restricted epitopes from CMV, EBV, and Influenza for use as a functional control in human immune monitoring studies

Julie S. Nielsen ^{a,b}, Darin A. Wick ^a, Eric Tran ^{a,c}, Brad H. Nelson ^{a,b,c,d}, John R. Webb ^{a,c,*}

^a *Trev and Joyce Deeley Research Centre, British Columbia Cancer Agency, Victoria, British Columbia, Canada*

^b *Department of Medical Genetics, University of British Columbia, Vancouver, British Columbia, Canada*

^c *Department of Biochemistry and Microbiology, University of Victoria, Victoria, British Columbia, Canada*

^d *Department of Biology, University of Victoria, Victoria, British Columbia, Canada*

ARTICLE INFO

Article history:

Received 20 April 2010

Received in revised form 24 June 2010

Accepted 7 July 2010

Available online xxxx

Keywords:

T cells

CMV

EBV

Influenza

Peptides

Cancer

Antigen presentation

ABSTRACT

Interest and activity in the areas of clinical immunotherapy and therapeutic vaccines are growing dramatically, thus there is a pressing need to develop robust tools for assessment of vaccine-induced immunity. CD8+ T cell immunity against specific antigens is normally measured by either flow cytometry using MHCtetramer reagents or via biological assays such as intracellular cytokine staining or ELISPOT after stimulation with specific peptide epitopes. However, these methodologies depend on precise knowledge of HLA-restricted epitopes combined with HLA typing of subjects. As an alternative approach, electroporation of antigen presenting cells (APC) with *in vitro*-transcribed mRNA (IVT-mRNA) encoding the antigen of interest bypasses the requirements for HLA typing and knowledge of specific epitopes. A current limitation of the IVT-mRNA technique is the lack of robust positive control RNAs to verify the efficacy of electroporation and to ensure that the electroporated APC retain the ability to stimulate T cells. Herein we describe an IVT-mRNA construct wherein all 32 HLA class I-restricted epitopes of the widely used CEF (Cytomegalovirus, Epstein-Barr Virus and Influenza Virus) positive control peptide pool have been genetically spliced together to generate a single polyepitope construct. Each epitope is flanked by three amino- and three carboxy-terminal amino acids from the original parent protein to facilitate proteolytic processing by the proteasome. Using cells obtained from a panel of normal healthy donors and cancer patients we report that dendritic cells, CD40-activated B cells, PHA blasts, and even tumor cells can be transfected with CEF polyepitope IVT-mRNA and can elicit robust CEF-specific responses from autologous T cells, as measured by IFN- γ ELISPOT. Moreover, the response elicited by CEF IVT-mRNA-transfected APC was similar in magnitude to the response elicited by the complete pool of CEF minimal peptide epitopes, implying that the polyepitope parent protein encoded by the CEF mRNA was efficiently processed into individual epitopes by the proteolytic machinery of the APC. In summary, the CEF polyepitope IVT-mRNA described herein comprises a robust positive control for immunomonitoring studies requiring IVT-mRNA transfection and potentially provides a unique tool for assessing MHC class I processing regardless of HLA haplotype.

Crown Copyright © 2010 Published by Elsevier B.V. All rights reserved.

1. Introduction

The number of clinical trials utilizing various forms of immunotherapy for treating infectious disease and cancer is growing rapidly. Although clinical endpoints vary widely and are trial-specific, immunomonitoring is often used to gauge

* Corresponding author. Trev and Joyce Deeley Research Centre, British Columbia Cancer Agency, Victoria, BC, Canada, V8R 6V5. Tel.: +1 250 519 5706; fax: +1 250 519 2040.

E-mail address: jwebb@bccancer.bc.ca (J.R. Webb).

clinical efficacy in terms of immune responsiveness. Furthermore, although great success has been achieved with vaccines that induce a humoral response, it is clear that many settings require induction of an effective CD8+ T cell response. Thus, development of appropriate tools to evaluate these responses is of utmost importance. Assessment of CD8+ T cell immunity is normally achieved using one of two approaches: 1) flow cytometry to directly visualize antigen-specific T cells that have been stained with MHC tetramer reagents, or 2) *in vitro* stimulation with candidate peptide epitopes followed by quantitation of reactive T cells using biological assays such as intracellular cytokine staining or ELISPOT. The use of MHC tetramer reagents is dependent upon prior knowledge of precise epitopes and their HLA restricting elements. Moreover, while overlapping peptide libraries can be used for *in vitro* stimulation, epitopes that bind specific class I alleles are frequently used when assessing large proteins due to cost limitations. Indeed, the vast majority of clinical immunomonitoring studies conducted to date have focused upon the measurement of CD8+ T cell responses that are restricted by the highly prevalent class I allele, HLA-A2.

In instances where pre-existing knowledge of epitopes is incomplete, the use of antigen presenting cells (APC) electroporated with *in vitro*-transcribed mRNA (IVT-mRNA) encoding the antigen of interest is becoming widely recognized as an alternative approach for eliciting antigen-specific T cell responses (Britten et al., 2004; Kreiter et al., 2007; Knights et al., 2009). IVT-mRNAs are translated into protein within the cell, and then individual epitopes are cleaved from the parent protein via the endogenous processing machinery, as would occur during natural MHC class I antigen processing. IVT-mRNAs encoding numerous antigens have been successfully electroporated into various types of APC including dendritic cells (DC) (Ponsaerts et al., 2002a; Bonehill et al., 2004; Artusio et al., 2006; Holtkamp et al., 2006), CD40-activated B cells (Van den Bosch et al., 2005; Mason et al., 2008), PHA-activated CD4+ T cells (Naota et al., 2006) and even bulk PBMC (Van Camp et al., 2010). These mRNA-transfected APC have been used to recall vaccine-induced responses *ex vivo*, and to prime *de novo* T cell responses both *in vitro* and *in vivo*. Indeed, mRNA-transfected autologous DC are now being investigated as a cancer vaccination strategy in a number of clinical settings (Smits et al., 2009). However, a current limitation of the IVT-mRNA technique is the lack of robust positive controls to verify the efficacy of electroporation and T cell stimulation.

In the present study, we have created an IVT-mRNA construct encoding the 32 different HLA class I-restricted epitopes of the widely used CEF (Cytomegalovirus, Epstein-Barr Virus and Influenza Virus) positive control peptide pool. These epitopes were genetically spliced together to create a CEF polyepitope construct. CEF peptides are restricted by HLA-A1, -A2, -A3, -A11, -A24, -A68, -B7, -B8, -B27, -B35, and -B44 and have been shown to elicit recall responses in up to 88% of individuals (Currier et al., 2002; Janetzki et al., 2008); thus they are widely utilized, in peptide form, as a positive control for immunomonitoring assays such as ELISPOT. We report herein that DC, CD40-activated B cells, PHA blasts, and even tumor cells electroporated with CEF polyepitope IVT-mRNA all elicited robust responses from autologous T cells as measured by IFN- γ ELISPOT assay. We

propose that this CEF polyepitope mRNA serves as an excellent positive control for *in vivo* and *in vitro* human studies involving IVT-mRNA transfection and also provides a unique tool to assess MHC class I processing in a variety of human cell types, regardless of HLA haplotype.

2. Materials and methods

2.1. Design of the pST1-Gateway vector

The IVT-mRNA plasmid pST1-Sig-DC-LAMP (De Keersmaecker et al., 2009) containing a BamHI cloning site at the boundary between the DC-LAMP signal sequence and transmembrane/cytoplasmic region, and the control plasmids pST1-Sig-MART-1-DC-LAMP and pGEM-eGFP were kindly provided by Dr. Kris Thielemans. The pST1-Sig-MART-1-DC-LAMP construct encodes full-length MART-1 (A27L), with the exception of the start and stop codons, cloned into pST1-Sig-DC-LAMP using the BamHI cloning site (unpublished). We modified the pST1-Sig-DC-LAMP plasmid (Fig. 1A) by incorporating a Gateway™ cassette in place of the BamHI cloning site to generate the destination vector pST1-Gateway (Fig. 1B), which allows for simple directional cloning using the Gateway™ system (Invitrogen). In addition to site-specific *attR1* and *attR2* recombination sequences, this cassette also encodes the *ccdB* gene (for negative selection of non-recombined plasmids) and the chloramphenicol resistance gene. In addition, the neomycin phosphotransferase gene in the pST1 backbone was replaced with an ampicillin resistance cassette to facilitate cloning from Gateway™ entry vectors (Fig. 1C; Invitrogen).

This new pST1-Gateway vector, in and of itself, provides a useful tool for easily cloning any given antigen into a vector to facilitate *in vitro* transcription of the sequence of interest flanked by the DC-LAMP targeting sequences. Use of the vector requires three simple steps. First, the target is amplified by PCR. The sequence of the forward primer should be 5'CACC XXX, where CACC facilitates directional cloning into the Gateway™ entry vector, pENTR/D-TOPO (Invitrogen) and XXX is the first codon of the sequence of interest. The sequence of the reverse primer should be 5'XXX, where XXX is the sequence complimentary to the last codon BEFORE the stop codon in the sequence of interest. By omitting the stop codon, the open reading frame encoding the DC-LAMP targeting sequences is maintained. In addition to the DC-LAMP sequences, the pST1-Gateway vector also encodes short flanking sequences surrounding the cloning site (18 N-terminal amino acids and 9 C-terminal amino acids). The second step involves simple cloning of the PCR product into pENTR/D-TOPO. The third step is recombination with the pST1-Gateway vector (Fig. 1C), using Gateway technology (Invitrogen).

2.2. In vitro transcription and mRNA transfection

The pST1-CEF plasmid was linearized after the poly(A) sequence with Pmel. The control plasmids pST1-Sig-DC-LAMP and pGEM-eGFP were linearized with NotI and Sapi, respectively. Linearization was confirmed by agarose gel electrophoresis of an aliquot of the restriction digest, and the QIAquick gel extraction kit (QIAGEN) was used for DNA

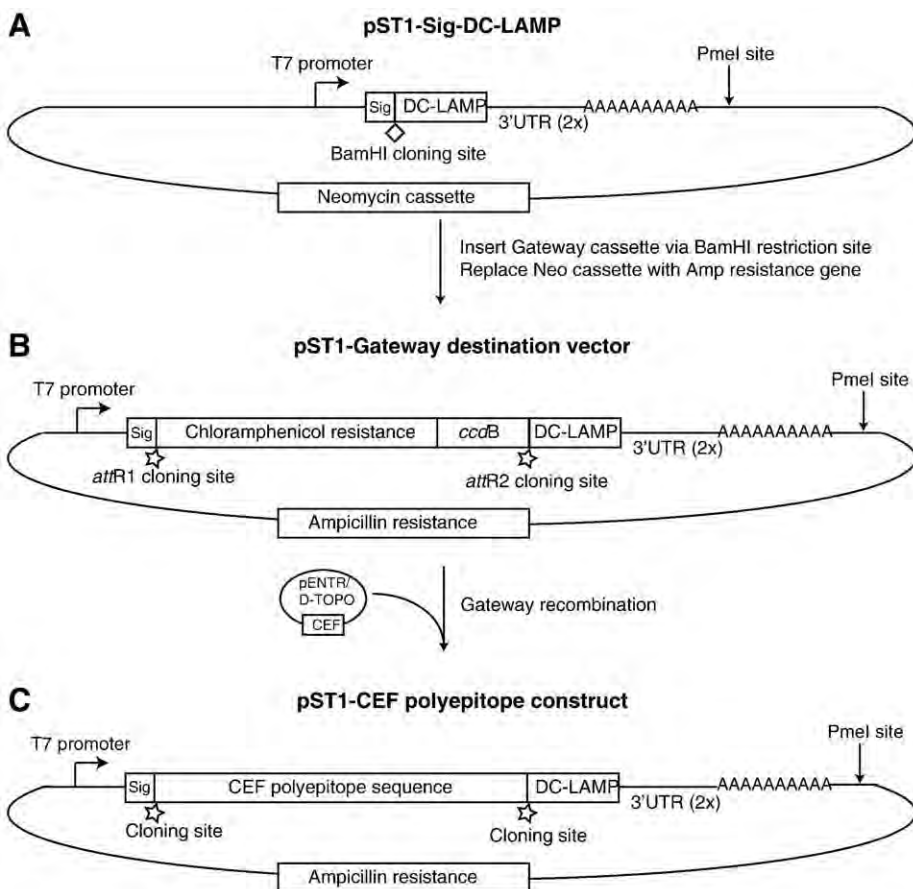


Fig. 1. Schematics of pST1-Gateway destination vector and CEF polyepitope construct. The CEF construct includes a T7 promoter for *in vitro* transcription of a single open reading frame with a signal sequence and targeting sequence from DC-LAMP flanking the CEF polyepitope sequence. This open reading frame is followed by two tandem 3'-UTRs and a 120 bp poly(A) sequence to increase RNA stability. Att sites (stars) facilitate cloning using the Gateway system, and a Pmel site enables linearization of the plasmid to increase transcription efficiency. Refer to Section 2.1 for additional details about the constructs.

cleanup of the remainder (without gel extraction). *In vitro* transcription of the linearized plasmid was performed using the mMessage mMachine T7 Ultra Kit (Ambion) as directed by the manufacturer. RNA integrity was confirmed by gel electrophoresis. B cells, PHA blasts, and tumor cells were transfected by electroporation using the Amaxa Human B Cell Nucleofection Kit (Lonza), and dendritic cells were transfected by electroporation using Optibuffer as previously described (Ponsaerts et al., 2002b) or using the Amaxa Human Dendritic Cell Nucleofection Kit (Lonza). Generally, 2×10^6 cells were transfected with 2 μ g of *in vitro*-transcribed mRNA.

2.3. Patient samples

All specimens and clinical data were obtained with informed consent under protocols approved by the Research Ethics Board of the British Columbia Cancer Agency and the University of British Columbia. Peripheral blood from patients and healthy donors was collected by venipuncture into sodium heparin tubes (BD Biosciences). PBMC were isolated by density centrifugation over Histopaque 1077 (Sigma) and then cryopreserved in liquid nitrogen vapor freezers. Ascites

was collected from ovarian cancer patients at the time of primary debulking surgery, and the ascites cellular component (AC) was collected by centrifugation and cryopreserved as described for PBMC.

2.4. Cells used for transfection

CD40-activated B cells were generated by culturing bulk PBMC with lethally irradiated (75Gy) CD40 ligand-expressing L cells (Caux et al., 1994) (kindly provided by Dr. John Gordon) at a 10:1 ratio. All B cells except IROL001 were cultured in complete IMDM media containing 10% human AB serum (Sigma), 10 mM HEPES, 2 mM L-glutamine, 50 μ M 2-mercaptoethanol, penicillin/streptomycin, 1 μ g/ml cyclosporin A, 2 ng/ml human IL-4 (Peprotech), and insulin-transferrin-sodium selenite for 2–4 weeks until cultures were >95% CD19+ as measured by flow cytometry. IROL001 B cells were cultured in complete RPMI 1640 containing 10% FBS, 2 mM L-glutamine, 50 μ M 2-mercaptoethanol, HEPES, sodium pyruvate, gentamicin, 1 μ g/ml cyclosporin A, and 2 ng/ml human IL-4. Monocyte-derived dendritic cells (MoDC) were generated by purifying CD14+ monocytes from PBMC using CD14 microbeads (Miltenyi, Biotec) according to the manufacturer's instructions and culturing cells in AIM-V media

with 160 ng/ml GM-CSF and 20 ng/ml recombinant human IL-4 for 5 days or from the adherent cell fraction of PBMC by culturing in complete RPMI with 200 ng/ml GM-CSF and 20 ng/ml recombinant human IL-4 for 4 days, followed by maturation with 10 ng/ml IL-1 β , 10 ng/ml TNF α , 1000 U/ml IL-6, and 1 μ g/ml PGE $_2$ for 2 days. Both strategies were effective for assessing CEF responses. PHA blasts were generated from ovarian cancer patient ascites cell preparations that were stimulated with 5 μ g/ml PHA in AIM-V media for 2 days, followed by AIM-V media with 100 IU/ml IL-2 for 3 days.

2.5. IFN- γ ELISPOT analyses

ELISPOT plates (MSIP, Millipore) were pre-coated overnight with 10 μ g/ml anti-IFN- γ capture antibody (1-D1K, Mabtech) and then blocked for 2 h at 37 °C with complete IMDM containing 10% human AB serum (DC017, DC027, IROC013 and IROC018 experiments), complete RPMI with 10% FBS (IROC008 DC and IROL001 experiments), or AIM-V (PHA blast experiments). Cryopreserved PBMC or ascites cells (AC) were thawed, and cells were plated on ELISPOT plates in triplicate at 2–3 \times 10 5 cells per well. Wells were supplemented with autologous APC (untreated or mock-transfected), autologous APC pulsed with CEF peptide pool (Anaspec), or autologous APC transfected with CEF IVT-mRNA or MART-1

IVT-mRNA, as indicated. Stimulation with PHA (5 μ g/ml) was used as a positive control for ELISPOT. After overnight incubation at 37 °C, ELISPOT plates were washed and incubated for 2 h at 37 °C with 1 μ g/ml biotinylated anti-human IFN- γ (mAB 7-B6-1, Mabtech) followed by developing with Vectastain ABC Elite kit and Vectastain AEC substrate reagent according to the manufacturer's instructions (Vector Labs). Spots were quantified by a commercial service provider (ZellNet Consulting, Inc), and results were reported as the number of spot forming cells per 10 6 bulk PBMC or AC.

3. Results

3.1. Design and preparation of the CEF polyepitope construct

A sequence-verified, synthetic DNA construct containing a single open reading frame encoding all 32 of the HLA Class I-restricted epitopes included in the widely used extended CEF peptide pool (Anaspec) was prepared by a contract service provider (Bionexus Inc.). Since the IVT-mRNA approach relies upon proteolytic processing of the translated sequence, we designed the construct to include, for each of the 32 epitopes, three amino-terminal and three carboxy-terminal flanking amino acids from the corresponding parent protein (see Table 1). The termini of the open reading frame were

Table 1

Sequences (including flanking amino acids) and HLA restriction of the 32 epitopes in the CEF polyepitope IVT-mRNA construct.

Epitope	Sequence ^{a,b}	HLA restriction
Influenza virus matrix protein M1 (58–66)	LTK <i>GILGFVFTL</i> TVP	HLA-A2
Influenza virus PA (46–54)	EVC <i>FMYSDFHF</i> I DER	HLA-A2
Influenza virus matrix protein M1 (13–21)	YVL <i>SIIPSGPLK</i> AEI	HLA-A3,A11
Influenza virus NP (342–351)	EDL <i>RVLSPFIKGTK</i> VVP	HLA-A3
Influenza virus NP (91–99)	DPK <i>KTGGPIYKR</i> VDG	HLA-A68
Influenza virus NP (418–426)	QRN <i>LPFDKTTVM</i> AAF	HLA-B7
Influenza virus NP (380–388)	STL <i>ELRSRYWAI</i> RTR	HLA-B8
Influenza virus NP (383–391)	ELR <i>SRYWAIRTTR <i>SGG</i></i>	HLA-B27
Influenza virus matrix protein M1 (128–135)	GAL <i>ASCMGLIY</i> NRN	HLA-B27
Epstein–Barr virus LMP2 (426–434)	VFM <i>CLGGLLTMV</i> AGA	HLA-A2
Epstein–Barr virus BMLF1 (280–288)	QNA <i>GLCTLVAML</i> EET	HLA-A2
Epstein–Barr virus latent NA3B (399–408)	GRP <i>AVFDRKSDAK</i> STK	HLA-A11
Epstein–Barr virus Rta protein (28–37)	LVS <i>DYCNVLNKEF</i> TAG	HLA-A24
Epstein–Barr virus BZLF-1 (190–197)	RKC <i>RAFKQQL</i> QHY	HLA-B8
Epstein–Barr virus NA-3A (337–347)	NAG <i>FLRGRAYGL</i> DLL	HLA-B8
Epstein–Barr virus NA-3A (158–166)	RRD <i>QAKWRLQTL</i> AAG	HLA-B8
Epstein–Barr virus NA-3C (258–266)	RRY <i>RRIYDIEL</i> CGS	HLA-B27
Epstein–Barr virus NA-3A (458–466)	GMA <i>YPLHEQHGM</i> APC	HLA-B35
Cytomegalovirus pp65 (495–503)	LAR <i>NLVPMPVATV</i> QGQ	HLA-A2
Cytomegalovirus pp65 (417–426)	ERK <i>TPRVTGGGAM</i> AGA	HLA-B7
Cytomegalovirus pp65 (378–389)	AEE <i>SDEEEAIVAYTL</i> ATA	HLA-B18
Cytomegalovirus pp65 (123–131)	MLN <i>IPSINVHHY</i> PSA	HLA-B35
Influenza virus PB1 (591–599)	GII <i>VSDGGPNLY</i> NIR	HLA-A1
Influenza virus NP (44–52)	IQM <i>CTELKLSDY</i> EGR	HLA-A1
Influenza virus NP (265–274)	SAL <i>ILRGSVAHK</i> SCL	HLA-A3
Epstein–Barr virus BRLF-1 (148–156)	KHS <i>RVRAYTYSK</i> VLG	HLA-A3
Epstein–Barr virus NA-3A (603–611)	RLA <i>RLRAEAQVK</i> QAS	HLA-A3
Epstein–Barr virus NA-3B (416–424)	CRA <i>IVTDFSVIK</i> AIE	HLA-A11
Epstein–Barr virus BRLF-1 (134–142)	MIP <i>ATIGTAMYK</i> LLK	HLA-A11
Epstein–Barr virus NA-3A (379–387)	KVK <i>RPPIFIRRL</i> HRL	HLA-B7
Epstein–Barr virus NA-3C (281–290)	LQT <i>EENLLDFVRF</i> MGV	HLA-B44
Cytomegalovirus pp65 (511–525)	KYQ <i>EFFWDANDIY</i> RIF	HLA-B44

^a Sequence shows minimal epitope (bold type) as well as 3 amino-terminal and 3 carboxy-terminal flanking amino acids (italics) from the naturally expressed parent protein.

^b Sequences are expressed as one contiguous open reading frame, in the order as shown, with no additional intervening sequences.

subsequently modified by PCR with the following primers (5' CACC ATG CTG ACC AAA GGT ATT CTG GGC3' and 5'AAA ATG GCG ATA GAT ATC GTT GGC3'). The CACC sequence at the 5' end of the forward primer facilitated directional cloning of the PCR product into the Gateway™ entry vector, pENTR/D-TOPO (Invitrogen) and subsequently into pST1-Gateway by site-specific recombination to generate the plasmid pST1-CEF, using the strategy and construct outlined in [Section 2.1](#) and [Fig. 1](#)). In order to be contiguous with the reading frame of the DC-LAMP signal sequence (upstream) through to the end of the DC-LAMP transmembrane/cytoplasmic region (downstream), the first codon of the CEF polyepitope insert was located immediately after the CACC of the forward primer, and the 5' end of the reverse primer encoded the final codon of the CEF sequence.

The resulting pST1-CEF construct enables *in vitro* transcription (via the T7 RNA polymerase promoter) of an mRNA that encodes the complete CEF polyepitope sequence in frame with a DC-LAMP signal sequence and a DC-LAMP transmembrane/cytoplasmic region ([Fig. 1C](#)). The mRNA also contains two tandem copies of the β-globin 3'-UTR and a 120 bp vector-encoded poly(A) sequence, reported to increase IVT-mRNA stability and translation efficiency ([Holtkamp et al., 2006](#)). The pST1-CEF construct was used as a template for *in vitro* transcription as described in [Materials and methods](#), which resulted in efficient and reliable production of full-length CEF mRNA (typical yields of approximately 35 µg of RNA from 2 µg of linearized plasmid using 4 µl T7 enzyme mix per reaction).

3.2. Validation of the CEF polyepitope construct

We validated the CEF polyepitope construct as a positive control for IVT-mRNA-based immunological studies by transfecting a variety of antigen presenting cells and measuring their ability to stimulate autologous T cells. We initially assessed the construct in CD40-activated primary human B cells isolated from two healthy donors (DC017 and DC027) as well as an ovarian cancer patient (IROC013) and a lymphoma patient (IROL001). B cells expanded from bulk PBMC by stimulation with CD40L-expressing L cells plus IL-4 were electroporated with CEF IVT-mRNA and used as antigen presenting cells in IFN-γ ELISPOT assays. In all 4 cases, CD40-activated B cells that had been transfected with CEF IVT-mRNA elicited robust activation of autologous T cells as measured by IFN-γ ELISPOT ([Fig. 2A](#)). Importantly, the number of spot forming cells in the presence of CEF mRNA-transfected B cells (600 to 1500 per 10⁶ PBMC) was essentially equivalent to the number of spot forming cells in the presence of exogenously added CEF peptides, suggesting that individual epitopes were efficiently processed from the mRNA-encoded CEF polyepitope parent protein. In contrast, minimal activation occurred in the presence of untransfected CD40-activated B cells or cells that had been electroporated with MART-1 (irrelevant antigen) IVT-mRNA.

Similar results were observed when monocyte-derived dendritic cells (MoDC) were transfected with CEF IVT-mRNA and used as an APC in IFN-γ ELISPOT assays ([Fig. 2B](#)). A range of responses against CEF epitopes was noted, including high responders (IROC008, DC022, and DC065), low responders (DC020, DC026, and DC067), and complete non-responders

(DC016 and DC068). Results using CEF IVT-mRNA-transfected MoDC were consistent with results using peptide-pulsed MoDC. The transfection efficiency was 79% and 99% for B cells and DC, respectively, as assessed by flow cytometry after transfection with GFP IVT-mRNA (measured in one experiment, data not shown). Viability after transfection was 75–80%.

Since CD40-activated B cells and dendritic cells are considered professional antigen presenting cells, we also investigated whether CEF IVT-mRNA could be efficiently expressed and processed in a non-professional antigen presenting cell. Recently, several groups have demonstrated that PHA-activated T cells can be transfected with IVT-mRNA ([Naota et al., 2006](#); [Van Camp et al., 2010](#)), providing a potentially rich and convenient source of antigen presenting cells from even minimal volumes of peripheral blood. In agreement with these reports, we found that CEF IVT-mRNA-transfected PHA blasts were also able to process and present CEF epitopes to autologous T cells ([Fig. 2C](#)). However, in 2 of 3 samples, the magnitude of the response elicited by CEF IVT-mRNA-transfected PHA blasts was only about 50% of the response elicited by exogenously added CEF peptides.

3.3. Use of the CEF polyepitope construct as a tool to test antigen processing and presentation capacity

Human tumor cells often harbor defects in antigen processing as an immune escape phenomenon. Therefore, in addition to its utility as a positive control for immunomonitoring assays, we reasoned that the CEF polyepitope construct might also be a universally applicable tool for assessing the integrity of antigen processing and presentation pathways in tumor cells, since all individuals are anticipated to harbor T cells specific to one or more epitopes in the construct. Defects in antigen processing and presentation in candidate tumor cells could readily be detected by transfecting tumor cells with CEF IVT-mRNA and assessing whether or not the cells successfully activate CEF-reactive T cells in autologous PBMC. As a proof-of-concept experiment, we transfected primary tumor cells derived from a serous ovarian cancer patient (IROC018) with CEF IVT-mRNA and assessed T cell activation by ELISPOT. We found that IVT-mRNA-transfected tumor cells activated T cells to the same extent as seen with exogenously added CEF peptides (which do not require functional antigen processing machinery). Furthermore, the response elicited by CEF IVT-mRNA-transfected tumor cells was similar to that elicited by transfected CD40-activated B cells from the same patient (albeit lower in tumor cells compared to B cells). Together these data indicate that the MHC class I antigen processing and presentation pathway was intact and functional in tumor cells from this particular patient ([Fig. 2D](#)).

4. Discussion

The extended CEF peptide pool is a collection of 32 known CD8 T cell epitopes from Cytomegalovirus, Epstein–Barr virus and Influenza virus that have been shown to elicit recall responses from the PBMC of up to 88% of individuals, regardless of HLA haplotype ([Currier et al., 2002](#); [Janetzki et al., 2008](#)). Thus the CEF peptide pool is widely used as a positive control to validate assay performance in

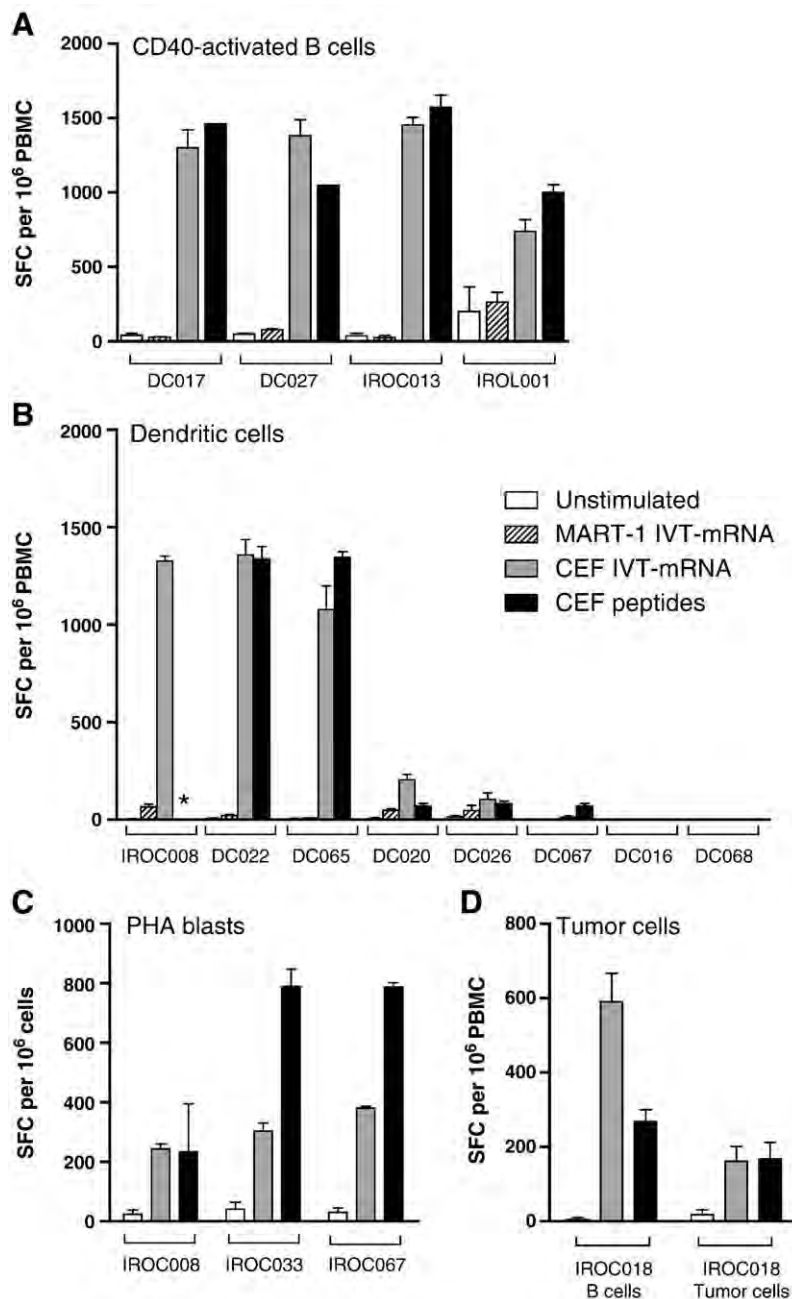


Fig. 2. APC transfected with CEF IVT-mRNA process and present CEF epitopes and activate T cells. IFN- γ ELISPOT assays comparing activation of T cells by APC incubated with CEF peptides or transfected with CEF IVT-mRNA or negative control MART-1 IVT-mRNA. A range of APC, responder cell numbers, and conditions were tested to ensure the robustness of the CEF IVT-mRNA system. Samples included cells from 2 healthy donor controls (DC017, DC027), 5 ovarian cancer patients (IROC008, IROC013, IROC018, IROC033, IROC067), and 1 follicular lymphoma patient (IROL001). (A) CD40-activated B cells (50,000/well) were left untransfected, electroporated with IVT-mRNA encoding MART-1 (negative control) or IVT-mRNA encoding the CEF polyepitope protein, or pulsed with a CEF peptide pool, and used as stimulators in an IFN- γ ELISPOT assay using autologous PBMC as responders. DC017 and DC027 were not assessed in triplicate with CEF peptides. (B) Monocyte-derived dendritic cells (12,500/well) were mock-transfected (no RNA) or electroporated with IVT-mRNA encoding MART-1 (negative control) or IVT-mRNA encoding the CEF polyepitope protein, or pulsed with the CEF peptide pool, and used as stimulators in an IFN- γ ELISPOT assay using autologous PBMC as responders. *CEF peptides not tested with IROC008. (C) PHA blasts (100,000/well) were mock-transfected (no RNA), electroporated with IVT-mRNA encoding the CEF polyepitope protein, or combined with the CEF peptide pool, and used as stimulators in an IFN- γ ELISPOT assay using bulk autologous ascites cells as responders. (D) Tumor cells or CD40-activated B cells (200,000/well) were left untransfected, electroporated with IVT-mRNA encoding the CEF polyepitope protein, or pulsed with a CEF peptide pool, and used as stimulators in an IFN- γ ELISPOT assay using autologous PBMC as responders. Results are reported as mean IFN- γ spot forming cells (SFC) + standard deviation for each sample assessed in triplicate.

immunomonitoring assays such as ELISPOT. To extend the use of the CEF peptide strategy to experiments involving IVT-mRNA transfection, we incorporated all 32 of the CEF

peptides into a single contiguous polyepitope construct contained in an optimized IVT-mRNA vector. We demonstrated that this construct, when transfected into APC from

multiple individuals, stimulates T cell responses of similar magnitude to those achieved with the CEF peptide pool. Thus, this construct can serve as a universal positive control for IVT-mRNA experiments.

IVT-mRNA methodology is growing in popularity as an approach for driving and measuring CD8+ T cell immunity, and is particularly useful in those instances where specific knowledge of HLA allele makeup and/or epitope sequence is unknown. In particular, the use of autologous dendritic cells transfected with tumor-associated antigen (TAA)-encoding mRNA has shown promise as an immunotherapeutic approach in a number of different oncology settings (Smits et al., 2009). DC transfected with IVT-mRNA exhibit efficient cytoplasmic expression of transgenes, excellent T cell priming capabilities and a superior clinical safety profile. Indeed, Good Manufacturing Practice (GMP) grade production of vaccines based upon autologous mRNA-electroporated dendritic cells has recently been described (Erdmann et al., 2007; Van Driessche et al., 2009). Expression of transfected IVT GFP mRNA is currently the most widely used positive control in this field and while this is useful for monitoring transfection efficiency, it does not give information about the functional status of transfected APC. In contrast, use of a CEF IVT-mRNA construct provides information about both transfection efficiency and APC functionality. Furthermore, like the CEF peptide pool, CEF IVT-mRNA is universally applicable to all patients, regardless of HLA haplotype, making it particularly useful for GMP-level protocols.

In addition to comprising an excellent control for IVT-mRNA systems, the CEF IVT-mRNA construct can also be used to assess antigen processing and presentation by a variety of cell types, including tumor cells. Although a number of different viral systems are used to study antigen processing in inbred strains of mice with defined MHC haplotypes, the same studies are challenging in humans due to the extreme heterogeneity of HLA loci. In that the CEF peptides comprise epitopes that are restricted by 11 different HLA class I alleles, they facilitate the use of essentially any donor PBMC as a source of cells for experimental purposes, since up to 88% of individuals will respond to the pool. In fact, we are not aware of any other such tool that can be used to universally study antigen processing in the human system. Importantly, T cells from all individuals that we have tested to date have responded robustly to CEF IVT-mRNA-transfected autologous antigen presenting cells, at levels similar to those evoked by CEF peptides themselves. Although we have not mapped CEF-specific T cell responses in these individuals at the level of specific peptides, it is likely that each individual would have a unique pattern of reactivity, based upon their HLA type and history of antigen exposure. Furthermore, since the ELISPOT response elicited by CEF peptides and CEF IVT-mRNA was generally similar for each donor, we speculate that each of the individual CEF peptides is likely cleaved from the parent protein with similar efficiency.

Proteolytic breakdown by the proteasome is an enzymatic process and the enzymes involved have defined substrate specificities (Kloetzel, 2004). Although C-terminal epitope ends are thought to be generated primarily in the proteasome (Mo et al., 1999), N-terminal processing is a more complex process (Yewdell and Bennink, 2001) involving post-proteasomal enzymes. Recently, a distinct N-terminal processing

motif was identified that was at least seven residues in length (Schatz et al., 2008). Clearly, this extensive flanking sequence is absent from each epitope in the CEF IVT-mRNA construct; therefore, it appears N-terminal processing can occur via an alternative mechanism. It may be that because we have artificially placed the CEF epitopes in tandem, the C-terminal end of the epitope that is immediately upstream may result in a short N-terminal extension (6 amino acids) that can be subsequently cleaved off via N-terminal trimming. Regardless of the precise mechanism, the majority of what is currently known about patterns of proteolytic processing has been gleaned, via necessity, from murine systems. Thus, the CEF IVT-mRNA system described herein provides a unique opportunity to address similar questions in the human system.

Moreover, the CEF IVT-mRNA polyepitope construct potentially provides a unique and universal tool to readily assess the integrity of the MHC class I processing pathway in human tumor cells. Immunological escape is known to play a critical role in cancer disease progression as evidenced by a plethora of different defects that are presumed to arise in the face of immunological pressure (Seliger, 2008). Because the CEF mRNA can elicit responses from a majority of individuals, it provides a unique opportunity to transfet a tumor cell line and then test for the ability of the transfected tumor cells to stimulate CEF-specific T cells present in autologous PBMC. By comparing with peptide-elicited responses, it may be possible to determine the underlying nature of any class I processing defects. For example, it may be possible to determine whether a defect is global in nature or whether it affects particular alleles and whether it is occurring at the intracellular (processing) level or extracellular (assembly) level. As proof of principle we have shown that tumor cells from an ovarian cancer patient can be readily transfected with CEF IVT-mRNA and can stimulate autologous PBMC at the same frequency as peptide-pulsed tumor cells, suggesting that in this tumor, the class I processing pathway is functional. This type of information could be crucial to the monitoring and interpretation of immunotherapy studies in cancer that depend upon recognition of class I-restricted epitopes.

In summary, we propose that this CEF IVT-mRNA system comprises a unique and powerful tool to study various aspects of MHC class I antigen processing in the human setting, and also comprises a useful positive control for investigators employing the IVT-mRNA platform for both T cell priming and recall experiments.

Acknowledgments

This work was supported by the British Columbia Cancer Foundation. J.S.N. is supported by a Canadian Institutes of Health Research Fellowship. The authors thank Kristy Dillon and Adam Girardin for technical assistance.

References

- Artusio, E., Hathaway, B., Stanson, J., Whiteside, T.L., 2006. Transfection of human monocyte-derived dendritic cells with native tumor DNA induces antigen-specific T-cell responses in vitro. *Cancer Biol. Ther.* 5, 1624.
- Bonehill, A., Heirman, C., Tuyaerts, S., Michiels, A., Breckpot, K., Brusse, F., Zhang, Y., Van Der Bruggen, P., Thielemans, K., 2004. Messenger RNA-

electroporated dendritic cells presenting MAGE-A3 simultaneously in HLA class I and class II molecules. *J. Immunol.* 172, 6649 (Baltimore, Md.).

Britten, C.M., Meyer, R.G., Frankenberg, N., Huber, C., Wolfel, T., 2004. The use of clonal mRNA as an antigenic format for the detection of antigen-specific T lymphocytes in IFN-gamma ELISPOT assays. *J. Immunol. Methods* 287, 125.

Caux, C., Massacrier, C., Vanbervliet, B., Dubois, B., Van Kooten, C., Durand, I., Banchereau, J., 1994. Activation of human dendritic cells through CD40 cross-linking. *J. Exp. Med.* 180, 1263.

Currier, J.R., Kuta, E.G., Turk, E., Earhart, L.B., Loomis-Price, L., Janetzki, S., Ferrari, G., Birx, D.L., Cox, J.H., 2002. A panel of MHC class I restricted viral peptides for use as a quality control for vaccine trial ELISPOT assays. *J. Immunol. Methods* 260, 157.

De Keersmaecker, B., Heirman, C., Allard, S., Bonehill, A., Corthals, J., Thielemans, K., Aerts, J.L., 2009. Luminal part of the DC-LAMP protein is not required for induction of antigen-specific T cell responses by means of antigen-DC-LAMP messenger RNA-electroporated dendritic cells. *Hum. Gene Ther.* 21, 479.

Erdmann, M., Dorrie, J., Schaft, N., Strasser, E., Hendelmeier, M., Kampgen, E., Schuler, G., Schuler-Thurner, B., 2007. Effective clinical-scale production of dendritic cell vaccines by monocyte elutriation directly in medium, subsequent culture in bags and final antigen loading using peptides or RNA transfection. *J. Immunother.* 30, 663.

Holtkamp, S., Kreiter, S., Selmi, A., Simon, P., Koslowski, M., Huber, C., Tureci, O., Sahin, U., 2006. Modification of antigen-encoding RNA increases stability, translational efficacy, and T-cell stimulatory capacity of dendritic cells. *Blood* 108, 4009.

Janetzki, S., Panageas, K.S., Ben-Porat, L., Boyer, J., Britten, C.M., Clay, T.M., Kalos, M., Maecker, H.T., Romero, P., Yuan, J., Kast, W.M., Hoos, A., 2008. Results and harmonization guidelines from two large-scale international Elispot proficiency panels conducted by the Cancer Vaccine Consortium (CVC/SVI). *Cancer Immunol. Immunother.* 57, 303.

Kloetzel, P.M., 2004. Generation of major histocompatibility complex class I antigens: functional interplay between proteasomes and TPPII. *Nat. Immunol.* 5, 661.

Knights, A.J., Nuber, N., Thomson, C.W., de la Rosa, O., Jager, E., Tiercy, J.M., van den Broek, M., Pascolo, S., Knuth, A., Zippelius, A., 2009. Modified tumour antigen-encoding mRNA facilitates the analysis of naturally occurring and vaccine-induced CD4 and CD8 T cells in cancer patients. *Cancer Immunol. Immunother.* 58, 325.

Kreiter, S., Konrad, T., Sester, M., Huber, C., Tureci, O., Sahin, U., 2007. Simultaneous ex vivo quantification of antigen-specific CD4+ and CD8+ T cell responses using in vitro transcribed RNA. *Cancer Immunol. Immunother.* 56, 1577.

Mason, N.J., Coughlin, C.M., Overley, B., Cohen, J.N., Mitchell, E.L., Colligon, T. A., Clifford, C.A., Zurbriggen, A., Sorenmo, K.U., Vonderheide, R.H., 2008.

RNA-loaded CD40-activated B cells stimulate antigen-specific T-cell responses in dogs with spontaneous lymphoma. *Gene Ther.* 15, 955.

Mo, X.Y., Cascio, P., Lemerise, K., Goldberg, A.L., Rock, K., 1999. Distinct proteolytic processes generate the C and N termini of MHC class I-binding peptides. *J. Immunol.* 163, 5851.

Naota, H., Miyahara, Y., Okumura, S., Kuzushima, K., Akatsuka, Y., Hiasa, A., Kitano, S., Takahashi, T., Yuta, A., Majima, Y., Shiku, H., 2006. Generation of peptide-specific CD8+ T cells by phytohemagglutinin-stimulated antigen-mRNA-transduced CD4+ T cells. *J. Immunol. Methods* 314, 54.

Ponsaerts, P., Van den Bosch, G., Cools, N., Van Driessche, A., Nijs, G., Lenjou, M., Lardon, F., Van Broeckhoven, C., Van Bockstaele, D.R., Berneman, Z.N., Van Tendeloo, V.F., 2002a. Messenger RNA electroporation of human monocytes, followed by rapid in vitro differentiation, leads to highly stimulatory antigen-loaded mature dendritic cells. *J. Immunol.* 169, 1669 (Baltimore, Md.).

Ponsaerts, P., Van den Bosch, G., Cools, N., Van Driessche, A., Nijs, G., Lenjou, M., Lardon, F., Van Broeckhoven, C., Van Bockstaele, D.R., Berneman, Z.N., Van Tendeloo, V.F., 2002b. Messenger RNA electroporation of human monocytes, followed by rapid in vitro differentiation, leads to highly stimulatory antigen-loaded mature dendritic cells. *J. Immunol.* 169, 1669.

Schatz, M.M., Peters, B., Akkad, N., Ullrich, N., Martinez, A.N., Carroll, O., Bulik, S., Rammensee, H.G., van Endert, P., Holzhueter, H.G., Tenzer, S., Schild, H., 2008. Characterizing the N-terminal processing motif of MHC class I ligands. *J. Immunol.* 180, 3210.

Seliger, B., 2008. Molecular mechanisms of MHC class I abnormalities and APM components in human tumors. *Cancer Immunol. Immunother.* 57, 1719.

Smits, E.L., Anguille, S., Cools, N., Berneman, Z.N., Van Tendeloo, V.F., 2009. Dendritic cell-based cancer gene therapy. *Hum. Gene Ther.* 20, 1106.

Van Camp, K., Cools, N., Stein, B., Van de Velde, A., Goossens, H., Berneman, Z. N., Van Tendeloo, V., 2010. Efficient mRNA electroporation of peripheral blood mononuclear cells to detect memory T cell responses for immunomonitoring purposes. *J. Immunol. Methods* 354, 1.

Van den Bosch, G.A., Ponsaerts, P., Nijs, G., Lenjou, M., Vanham, G., Van Bockstaele, D.R., Berneman, Z.N., Van Tendeloo, V.F., 2005. Ex vivo induction of viral antigen-specific CD8 T cell responses using mRNA-electroporated CD40-activated B cells. *Clin. Exp. Immunol.* 139, 458.

Van Driessche, A., Van de Velde, A.L., Nijs, G., Braeckman, T., Stein, B., De Vries, J.M., Berneman, Z.N., Van Tendeloo, V.F., 2009. Clinical-grade manufacturing of autologous mature mRNA-electroporated dendritic cells and safety testing in acute myeloid leukemia patients in a phase I dose-escalation clinical trial. *Cytotherapy* 11, 653.

Yewdell, J.W., Bennink, J.R., 2001. Cut and trim: generating MHC class I peptide ligands. *Curr. Opin. Immunol.* 13, 13.